

PAPER • OPEN ACCESS

BBN bounds on neutrinophilic ultralight Dark Matter

To cite this article: T. Bertólez-Martínez *et al* JCAP02(2026)039

View the [article online](#) for updates and enhancements.

You may also like

- [A systematic study of light dependency of persistent photoconductivity in a-InGaZnO thin-film transistors](#)
Yalan Wang, , Mingxiang Wang et al.
- [Bulk and interface quantum states of electrons in multi-layer heterostructures with topological materials](#)
Aleksandar Nikolic, Kexin Zhang and C H W Barnes
- [First principles study of interactions of oxygen-carbon-vacancy in bcc Fe](#)
Yuan You, , Mu-Fu Yan et al.

BBN bounds on neutrinophilic ultralight Dark Matter

T. Bertólez-Martínez ^a, J. López-Sarrión ^b and J. Salvado ^a

^a*Departament de Física Quàntica i Astrofísica and Institut de Ciències del Cosmos,
Universitat de Barcelona,
Diagonal 647, E-08028 Barcelona, Spain*

^b*Departamento de Física Teórica and Centro de Astropartículas y Física de Altas Energías (CAPA),
Universidad de Zaragoza,
Zaragoza 50009, Spain*

E-mail: antoni.bertolez@fqa.ub.edu, justo.lopezsarrion@gmail.com,
jsalvado@icc.ub.edu

ABSTRACT: The high densities in the early Universe provide a unique laboratory to constrain couplings between feebly interacting particles, such as dark matter and neutrinos. In this article, we study how Big Bang Nucleosynthesis can constrain models of Ultra-Light Dark Matter diagonally coupled to neutrinos. We follow an adiabatic formalism which allows to average-out the rapid oscillations of the Dark Matter field and consistently take into account the feedback between the neutrino and the Dark Matter fields. This feedback alters the early Universe dynamics, causing the Dark Matter energy density to scale as radiation, while the neutrino mass scales as a^{-1} . These two effects modify primordial element abundances by modifying interaction rates and the expansion rate during nucleosynthesis. Then, we use primordial abundances to obtain leading cosmological bounds on the coupling in the range $m_\phi/\text{eV} \in (10^{-22}, 10^{-17})$, namely $g \lesssim 0.13(m_\phi/\text{eV})$ for $m_\phi \gtrsim 3 \times 10^{-20}$ eV and $g \lesssim 1.8 \times 10^{-11} \sqrt{m_\phi/\text{eV}}$ for $m_\phi \lesssim 3 \times 10^{-20}$ eV. This consistent cosmological treatment emphasizes that, in the mass interval where its physical assumptions hold, neutrino masses cannot be generated refractively by a direct coupling with an Ultra-Light Dark Matter field.

KEYWORDS: cosmological neutrinos, neutrino properties, dark matter theory, big bang nucleosynthesis

ARXIV EPRINT: [2509.22867](https://arxiv.org/abs/2509.22867)

Contents

1	Introduction	1
2	Formalism	2
2.1	Fermionic equation of motion	3
2.2	Pseudoscalar equation of motion	4
2.3	Adiabatic approximation	5
3	Cosmological evolution	7
3.1	Energy density and effective mass	7
3.2	Pressure and equation of state	9
3.3	Initial conditions	11
3.4	Massive neutrinos and N_{eff}	13
4	Big Bang Nucleosynthesis	14
5	Results and discussion	17
6	Conclusions and outlook	18
A	Details on the formalism	21
A.1	Solutions to the equations of motion	21
A.2	Evolution of the distribution function	22
A.3	Derivation of the adiabatic invariant	23

1 Introduction

The nature and properties of Dark Matter (DM) remain elusive. In the hope of shedding light into the darkness, particle physics, astrophysics, and cosmology have managed to greatly constrain the portals that can connect the dark sector of DM with the SM [1–4]. One of such possibilities is through the neutrino portal, i.e., the possibility that DM is neutrinophilic and only interacts with the SM through neutrinos. For instance, on the theory side such interactions are motivated by many models which predict a connection between the origin of non-zero neutrino masses and the nature of DM [5, 6]. However, due to the elusive nature of neutrinos, current experimental and observational constraints on ν -DM couplings are much weaker than their electromagnetic counterparts [7]. This motivates the search for new phenomenological approaches which can constrain them.

One particularly interesting candidate to DM are light scalar fields, which are predicted by many extensions to the SM [8–14]. Since they could be non-thermally produced through the misalignment mechanism –where the initial (random) value of the field is displaced from zero– [2, 15–18], these bosons could make up for the entirety of DM. When these bosons have mass $m_\phi \ll 1$ eV, namely $m_\phi \sim 10^{-22} - 10^{-10}$ eV, they are called Ultra-Light Dark Matter (ULDM) candidates, and have their own distinct phenomenology [2, 18–33].

The unconstrained properties of neutrinos and DM make ν -ULDM interactions span a wide range of interesting phenomenology, from distorted neutrino oscillations to high-energy astrophysics [34–71]. One of the main interests of these interactions is that neutrinos acquire

a mass by propagating through a medium of ULDM. Hence, these models might be able to provide a joint explanation for neutrino masses and dark matter [35, 66, 72, 73]. Since the DM number density increases in the early Universe as a^{-3} , these models predict a varying neutrino mass with $m_\nu \sim a^{-3/2}$. If one then requires neutrino masses to have the right order of magnitude in terrestrial oscillation experiments, then this predicts $m_\nu \sim 10$ eV in the CMB epoch. As discussed in [66, 67], this naive estimate motivates that the interaction is mediated by a light fermion mediator, which allows surpassing cosmological bounds.

However, since cosmology is not directly sensitive to the neutrino mass [74], this naive estimate must be refined in order to better understand when are such mediators necessary. To achieve that, one must understand the coupled evolution of neutrinos and ULDM, and follow the evolution of its energy density and pressure. For instance, if neutrinos acquire a mass when the amplitude of ULDM increases, this is an energy expense which modifies the dynamics of ULDM [56, 59]. As shown in [56], this modifies the neutrino mass scaling to $m_\nu \sim a^{-1}$.

In this work, we consistently study the cosmological implications of a coupling between Dirac neutrinos (ψ) and the ULDM field (ϕ). We do so through a pseudoscalar coupling, $ig\bar{\psi}\gamma^5\phi\psi$ [75, 76], which predicts mass-varying neutrinos with no coherent long-range interactions; but most results also apply to an scalar coupling. Then, we quantitatively compute the background evolution of the coupled field, accounting for the fast oscillations of the ULDM with an adiabatic approximation. Apart from modifying the scaling of m_ν , this full calculation predicts additional relativistic degrees of freedom in the early Universe. The effect of these two phenomena on primordial element abundances from Big Bang Nucleosynthesis can constrain the properties of the coupled ν -ULDM fluid and, thus, their coupling.

The outline of this article is as follows. In section 2, we introduce the action for the model and derive the equations of motion for both species. In section 2.3, we introduce the adiabatic approximation, a necessary ingredient to solve the equation of motion for an ULDM field. In section 3, we describe the cosmological implications of this model and its phenomenological signatures. In particular, in section 4 we discuss its effects on Big Bang Nucleosynthesis (BBN). Finally, in section 5 we present our results and in section 6 we conclude.

2 Formalism

We consider the following action in a curved spacetime background [77]

$$\begin{aligned} S &= \int \sqrt{-\det g} d^4x \mathcal{L}(x) \\ &= \int \sqrt{-\det g} d^4x \left(-\frac{1}{2} D_\mu \hat{\phi} D^\mu \hat{\phi} - \frac{1}{2} m_\phi^2 \hat{\phi}^2 + \bar{\psi} [i\not{D} - m_0 + ig\hat{\phi}\gamma^5] \psi \right). \end{aligned} \quad (2.1)$$

Here, \mathcal{L} is the Lagrangian density of the model, D_μ is a covariant derivative, $\det g$ is the metric determinant, $\bar{\psi} = \psi^\dagger \gamma^0$, m_ϕ is the bare mass of the pseudoscalar field, m_0 the bare mass of the neutrino field and g the coupling between both fields. Naively, gauge invariance asks that a coupling must exist both to electrons and to neutrinos. However, the coupling to electrons can be suppressed, for instance, if the ultralight pseudoscalar is coupled to an SM-singlet right-handed neutrino [35, 37]. Then, in this work ψ can safely refer to active neutrinos only. As a first step, we choose a diagonal coupling, which will not lead to modified neutrino oscillations.

From eq. (2.1), the equations of motion for the quantum fields are

$$-D^\mu D_\mu \hat{\phi} + m_\phi^2 \hat{\phi} = ig\bar{\psi}\gamma^5\psi, \quad (2.2)$$

$$i\not{D}\psi - (m_0 - ig\hat{\phi}\gamma^5)\psi = 0. \quad (2.3)$$

Within a cosmological framework, the occupation number of the pseudoscalar field $\hat{\phi}$ is large, and it can be described by a coherent state. The fermion field ψ can be described as an ensemble of classical particles with a given momentum \vec{p} . In this framework, every quantum operator \hat{O} is replaced by its expectation value [78]

$$\langle \hat{O} \rangle = \sum_s \int dP_1 dP_2 dP_3 \frac{1}{\sqrt{-\det g}} \frac{1}{2P^0} f(P, x, s) \langle \phi, P^s | \hat{O} | \phi, P^s \rangle. \quad (2.4)$$

P^μ are the conjugate momenta to the positions x^i which solve the geodesic equation, s is the spin and $f(P, x, s)$ the distribution function. $|\phi, P^s\rangle = |\phi\rangle \otimes |P^s\rangle$ is the product of a coherent state with field ϕ and a one-particle fermion state. Appendix A gathers the formal definitions for these states.

2.1 Fermionic equation of motion

We first analyze the equation of motion of fermions, eq. (2.3), where for now we treat ϕ as a constant and homogeneous value. As discussed later, this is a very good approximation for ultralight fields as the one under consideration. We perform the chiral rotation

$$\psi \rightarrow e^{i\alpha\gamma^5} \psi = (\cos\alpha + i\gamma^5 \sin\alpha) \psi, \quad (2.5)$$

where α is a constant parameter. The equation now becomes

$$(i\not{D} - (m_0 \cos\alpha - g\phi \sin\alpha) + i\gamma^5(-m_0 \sin\alpha + g\phi \cos\alpha)) \psi = 0, \quad (2.6)$$

where we have used $(\gamma^5)^2 = \mathbb{I}_4$, the 4x4 identity matrix. Now, by making the right choice,

$$\tan 2\alpha = \frac{g\phi}{m_0}, \quad (2.7)$$

we convert this equation into

$$(i\not{D} - m_\nu) \psi = 0. \quad (2.8)$$

This is the standard Dirac equation with a mass term given by

$$m_\nu = \sqrt{m_0^2 + g^2\phi^2}. \quad (2.9)$$

Now, this tells us that the eigenstates to the Dirac operator from eq. (2.3) are two states with the same mass, m_ν . The same result would have been achieved by directly doing the change of variables in the Lagrangian. The plane wave solutions to eq. (2.3) are

$$u^s(\vec{p}) = e^{i\alpha\gamma^5} u_0^s(\vec{p}), \quad v^s(\vec{p}) = e^{i\alpha\gamma^5} v_0^s(\vec{p}), \quad (2.10)$$

where $u_0^s(\vec{p}), v_0^s(\vec{p})$ are the plane wave solutions for a free fermion of mass m_ν . These solutions fulfill,

$$\bar{u}^s(\vec{p})\gamma^5 u^r(\vec{p}) = -\bar{v}^s(\vec{p})\gamma^5 v^r(\vec{p}) = 2ig\phi \delta^{sr}. \quad (2.11)$$

The chiral rotation of the Dirac eigenstates rotates the electroweak vertex with a global phase and thus scattering amplitudes are not modified.

Two main differences appear if neutrinos are coupled to the ULDM field through a scalar term $g\bar{\psi}\phi\psi$. On the one hand, the effective neutrino mass has a different dependence, $m_\nu = m_0 + g\phi$ [78–80]. However, in the early Universe, neutrino mass is dominated by $g\phi$, and so the scalar and pseudoscalar equally predict $m_\nu^2 \sim g^2\phi^2$. For example, for $m_0 \sim 10^{-3}$ eV, this happens at redshift $z \gg 150$. On the other hand, long-range self-interactions in the pseudoscalar coupling are spin-dependent and thus irrelevant, while self-interactions in the scalar coupling are important when $gm_0/m_\phi \gtrsim 10$ [78]. For $m_0 \lesssim 10^{-3}$ eV, couplings probed here make self-interactions also negligible in the scalar formalism (see figure 10). As a consequence, quantitative results shown in section 5 also apply to the scalar coupling. However, the formalism introduced here is not applicable to the scalar coupling at late time, where the mass dependence is different.

2.2 Pseudoscalar equation of motion

Now, we take the expectation value of eq. (2.2) assuming an homogeneous background field $\phi = \phi(t)$ and a collection of particles as in eq. (2.4), which leads to

$$-D_\mu D^\mu \phi + m_\phi^2 \phi = ig \sum_s \int dP_1 dP_2 dP_3 \frac{1}{\sqrt{-\det g}} \frac{1}{2P^0} f(P, x, s) \langle P^s | \bar{\psi} \gamma^5 \psi | P^s \rangle. \quad (2.12)$$

If $f(P, x, s) = f(P, x)$ is spin-independent and the same for particles and antiparticles, and working in the comoving momentum q as defined in [81], this gives

$$\ddot{\phi} + 3H\dot{\phi} + m_\phi^2 \phi = -2g^2 \phi \mathbf{g} a^{-2} \int 4\pi dq q^2 \frac{1}{\sqrt{q^2 + a^2(m_0^2 + g^2\phi^2)}} f_0(q), \quad (2.13)$$

where $f_0(q)$ is the Fermi-Dirac distribution,

$$f_0(q) = \frac{1}{(2\pi)^3} \frac{1}{e^{q/T_0^\nu} + 1}, \quad (2.14)$$

T_0^ν the neutrino temperature today and \mathbf{g} the number of fermionic internal degrees of freedom: particles and antiparticles, and both spins.

Here, there are three characteristic timescales,

- the cosmological time, H^{-1} , which controls the Hubble friction term and the rate at which $f_0 = f_0(q)$ changes ($\frac{df_0}{dt} = H \frac{df_0}{d \log q}$).
- the characteristic oscillation time of ϕ . Naively, given by m_ϕ , but might be modified by the interactions.
- the timescale of neutrino dynamics, controlled by $E_p = \sqrt{\vec{p}^2 + m_0^2 + g^2\phi^2}$.

The interplay of these three scales defines the necessary physical assumptions. In the one hand, the energy of neutrinos (whether it is kinetic or the rest mass) is always $E_p \gtrsim T_{\nu,0} \sim 10^{-4}$ eV. Even after neutrino feedback, for $m_\phi \lesssim 10^{-17}$ eV, we always have $E_p \gg m_\phi$. Consequently, fermion dynamics are much faster than the oscillation of ϕ . Taking ϕ to be constant during fermion dynamics, as done in the previous subsection, is valid. The same argument holds for electroweak interactions, with timescales GeV^{-1} . Furthermore, the homogeneity of the early Universe allows us to neglect any spatial variations of ϕ .

On the other hand, ULDM is obtained in the regime $m_\phi \gg H$, such that the field oscillates in scales much shorter than the cosmological expansion. In this limit, oscillations of ϕ are averaged-out, and thus ϕ can be understood as a collection of CDM particles [2]. However, in order to follow the dynamics of the interaction between the field and the fermions, e.g., see if fermions backreact in the dynamics of the field; an adiabatic approximation is required to rigorously average the oscillations out [82].

2.3 Adiabatic approximation

In the framework of the adiabatic approximation, we define two different time variables. First, the slow cosmological timescale H^{-1} is parametrised by the scale factor a . Second, the timescale of the field oscillation is parametrised with a proper time t . During an oscillation of ϕ (of timescale t), the scale factor a can be held constant, i.e. $a' = 0$. Thus, the equation of motion for ϕ becomes

$$\ddot{\phi} + m_\phi^2 \phi = -2g^2 \phi \mathbf{g} a^{-2} \int 4\pi dq q^2 \frac{1}{\sqrt{q^2 + a^2(m^2 + g^2\phi^2)}} f_0(q). \quad (2.15)$$

This is the equation of a one-dimensional non-relativistic particle moving on a potential well. The adiabatic approximation assumes that the real motion of ϕ is well described by assuming a constant in a complete period of oscillation t_ϕ .

In the adiabatic approximation, every observable \mathcal{O} at cosmological timescales is replaced by its value averaged over the oscillation,

$$\langle \mathcal{O} \rangle = \frac{1}{t_\phi} \int_0^{t_\phi} dt \mathcal{O}(\phi(t), \dot{\phi}(t)) = \frac{1}{t_\phi} \oint d\phi \frac{\mathcal{O}(\phi, \dot{\phi}(\phi))}{\dot{\phi}(\phi)}, \quad (2.16)$$

where \oint marks an integral over an oscillation of ϕ , of period

$$t_\phi = \int_0^{t_\phi} dt = \oint \frac{d\phi}{\dot{\phi}(\phi)}. \quad (2.17)$$

The period of oscillation would then define an oscillation frequency which we can interpret as an effective mass, $M_\phi = 2\pi/t_\phi$. The total energy density is given by

$$\rho(a, t) = \frac{1}{2} \dot{\phi}^2 - \frac{1}{2} m_\phi^2 \phi^2 + \rho_\nu(a, \phi). \quad (2.18)$$

This is similar to the standard ULDM scenario, but with an additional term accounting for the energy in the fermion sector,

$$\rho_\nu(a, \phi) = a^{-4} \mathbf{g} \int 4\pi dq q^2 \sqrt{q^2 + a^2(m_0^2 + g^2\phi^2)} f_0(q). \quad (2.19)$$

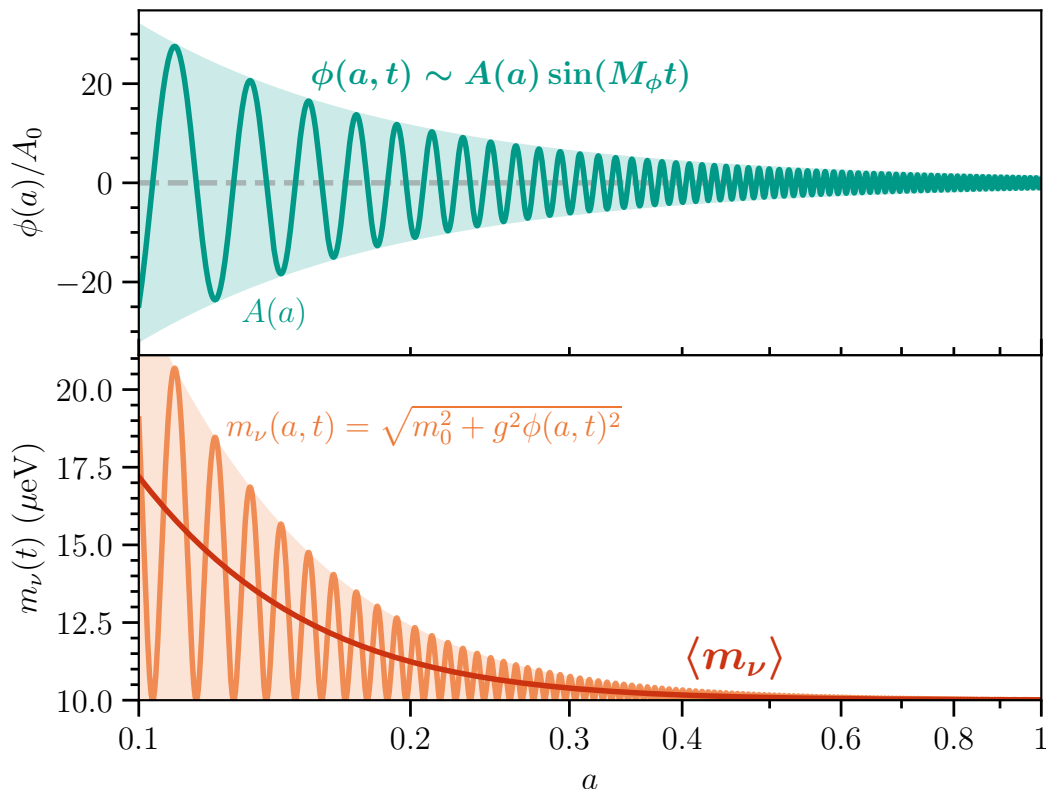


Figure 1. Illustration of the adiabatic approximation method. The top plot shows how the ULDM field $\phi(a, t)$ is oscillating rapidly around zero with amplitude $A(a)$ and frequency M_ϕ . As a consequence of the oscillating field, the bottom plot shows how the mass of the neutrino, $m_\nu(a, t)$, also oscillates rapidly with time. The adiabatic approximation allows to compute the averaged neutrino mass, $\langle m_\nu \rangle$, or the average of any other observable \mathcal{O} as in eq. (2.16). Curves here correspond to $m_0 = 10 \mu\text{eV}$, $g = 1.5 \times 10^{-20}$ and $m_\phi = 10^{-19} \text{eV}$, and $A_0 \equiv A(a = 1)$. For illustration purposes, the shown oscillation frequency is reduced by $\mathcal{O}(10^{21})$ compared to M_ϕ .

Within an oscillation we can treat the total energy as a constant of motion, $\rho(a, t) \simeq \langle \rho(a, t) \rangle \equiv \rho(a)$. This allows us to use eq. (2.18) to find a closed expression for $\dot{\phi}$,

$$\dot{\phi} = \sqrt{2} \sqrt{\rho(a) - m_\phi^2 \phi^2 / 2 - \rho_\nu(\phi)} \quad (2.20)$$

The adiabatic approximation formalism leads to the result that

$$\mathcal{I}(a) \equiv \frac{1}{\sqrt{2}} a^3 t_\phi \langle \dot{\phi}^2 \rangle = a^3 \oint d\phi \sqrt{\rho(a) - \frac{1}{2} m_\phi^2 \phi^2 - \rho_\nu(\phi)}, \quad (2.21)$$

is an invariant quantity for the whole cosmological evolution, i.e., $d\mathcal{I}/da = 0$. This adiabatic invariant allows us to compute the total energy density $\rho(a)$ of the system as a function of the scale factor, given some initial conditions. The derivation of this result is presented in appendix A.

Instead of $\rho(a)$, we work in terms of the amplitude of oscillations of the pseudoscalar, $A(a)$. In particular, $\phi = A$ is reached when $\dot{\phi} = 0$, and thus

$$\rho(a) = \frac{1}{2} m_\phi^2 A(a)^2 + \rho_\nu(a, A(a)). \quad (2.22)$$

Then, eq. (2.21) allows to compute the evolution of $A(a)$. In the $g \rightarrow 0$ limit, the adiabatic invariant becomes

$$\mathcal{I}(a) = a^3 \oint d\phi \sqrt{\frac{1}{2} m_\phi^2 (A^2 - \phi^2)} = \frac{\pi}{2} m_\phi a^3 A^2, \quad (2.23)$$

which means that $A(a) \sim a^{-3/2}$. As expected, in the $g \rightarrow 0$ limit ϕ behaves as CDM, with $\rho(a) \sim a^{-3}$. In the limit where the interaction potential dominates, i.e., $m_\phi^2 A^2 \ll \rho_\nu(a, A(a))$, the adiabatic invariant becomes

$$\mathcal{I}(a) = a \oint d\phi \sqrt{\mathfrak{g} \int 4\pi q^2 dq \left(\sqrt{q^2 + g^2 a^2 A^2} - \sqrt{q^2 + g^2 a^2 \phi^2} \right)} f_0(q). \quad (2.24)$$

By changing variables to $\tilde{\phi} = a\phi$, one can check that $\mathcal{I}(a, A) = \mathcal{I}(aA)$, thus $aA = \text{constant}$. In the limit where the interaction potential dominates, the pseudoscalar field does not scale like CDM, but following $A(a) \sim a^{-1}$. This is due to the neutrino-dominated potential having a different scaling dependence to the m_ϕ potential. Let us look into this further.

3 Cosmological evolution

Now that the adiabatic approximation fully follows the bidirectional feedback between the neutrino sector and the ULDM field, in this section we compute important cosmological variables affected by the interaction. All the shown results are computed in a modified version of CLASS [83–86] which implements the full adiabatic approximation method.

3.1 Energy density and effective mass

From the energy-momentum tensor,

$$\rho(a) = \langle \rho(a, t) \rangle = \frac{1}{2} \langle \dot{\phi}^2 \rangle + \frac{1}{2} m_\phi^2 \langle \phi^2 \rangle + \langle \rho_\nu(a, \phi) \rangle \equiv \frac{1}{2} \langle \dot{\phi}^2 \rangle + \langle V(\phi) \rangle, \quad (3.1)$$

which coincides with eq. (2.22), and the pseudoscalar potential is

$$V(\phi) = \frac{1}{2} m_\phi^2 \phi^2 + \rho_\nu(a, \phi). \quad (3.2)$$

The shape and scaling of this potential at different epochs are shown in figure 2. Firstly, $m_\phi^2 \phi^2$ is a quadratic potential, which scales as a^{-3} if ϕ behaves as standard CDM. Secondly, $\rho_\nu \sim a^{-4}$. Then, at some point in the past, defined as a_{tr} in figure 2, ρ_ν dominates and $V(\phi)$ changes scaling from a^{-3} to a^{-4} , while still being quadratic. Finally, if $gA \gg |\vec{p}|$, neutrinos can become non-relativistic, and then $V(\phi)$ becomes linear at large ϕ . The couplings required for this scenario are ruled out from the bounds obtained in section 5.

In a first approximation, we can assume that the linear momentum of neutrinos is much larger than their instantaneous mass, i.e., $T_\nu \gg gA$. We will refer to this regime as the linearised regime. In this limit, we can expand ρ_ϕ up to first order in ϕ and get

$$\rho(a, t) = \frac{1}{2} \dot{\phi}^2 + \frac{1}{2} m_\phi^2 \phi^2 + \frac{1}{2} \delta m_\phi^2 \phi^2 + \rho_\nu(a, 0), \quad (3.3)$$

where

$$\delta m_\phi^2 = 2 \left. \frac{\partial \rho_\nu(a, \phi)}{\partial \phi^2} \right|_{\phi=0} = a^{-2} g^2 \mathfrak{g} \int 4\pi dq q^2 \frac{1}{\sqrt{q^2 + a^2 m_0^2}} f(q) \quad (3.4)$$

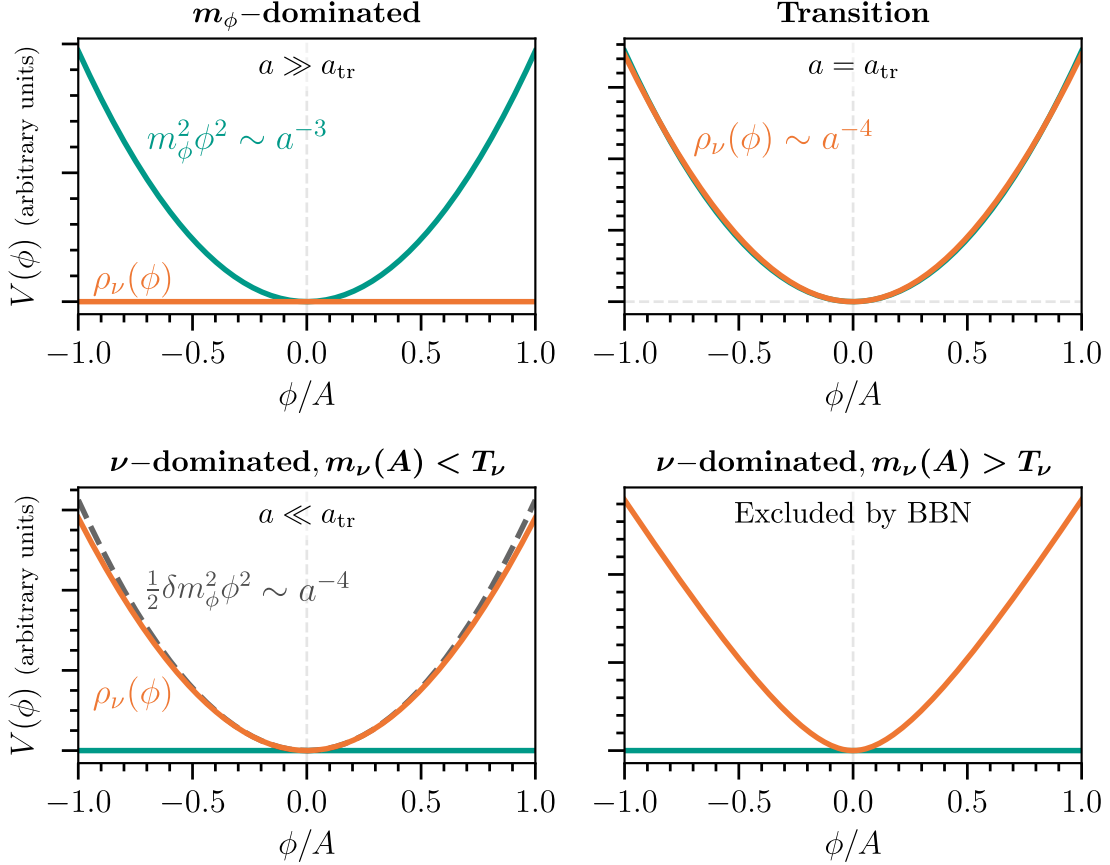


Figure 2. Evolution of the potential as in eq. (3.2). Left to right, top to bottom goes back in time. Today, the effect of neutrino interactions is negligible, and $V(\phi) = m_\phi^2 \phi^2 / 2$. However, $\rho_\nu(\phi)$ scales as a^{-4} , and therefore at some point ($a = a_{\text{tr}}$) in the past the neutrino potential equals the bare- m_ϕ potential. From that time on, $V(\phi) \sim a^{-4}$ and the scaling of $A(a)$ changes. If the momentum of neutrinos is larger than their effective mass, the $V(\phi)$ is quadratic, but if it becomes comparable, $V(\phi)$ becomes linear at large ϕ .

is an effective pseudoscalar mass from the energy expense necessary to provide neutrinos their mass. This effective mass scales as $\delta m_\phi^2 \sim a^{-2}$, as follows. The energy of a single neutrino coupled to ϕ , when $T_\nu \gg gaA \gg m_0$, is

$$E_p = \sqrt{\vec{p}^2 + m_0^2 + g^2 \phi^2} \simeq |\vec{p}| + \frac{g^2 \phi^2}{2|\vec{p}|}, \quad (3.5)$$

which implies an increment in energy $\sim g^2 \phi^2 / |\vec{p}|$. For fixed ϕ , this scales as $\sim a$, but the number density of neutrinos which receive the mass scales with a^{-3} . Thus, $\delta m_\phi^2 \sim a^{-2}$.

Then, the total effective mass of the pseudoscalar field is given by

$$M_\phi^2 = 2 \left. \frac{\partial^2 V(\phi)}{\partial \phi^2} \right|_{\phi=0} = m_\phi^2 + \delta m_\phi^2 \sim \begin{cases} m_\phi^2 \sim \text{constant} & a > a_{\text{tr}} \\ \delta m_\phi^2 \sim a^{-2} & a < a_{\text{tr}} \end{cases}, \quad (3.6)$$

where a_{tr} is quantitatively defined through $m_\phi^2 = \delta m_\phi^2$,

$$a_{\text{tr}}^2 = \frac{g^2}{m_\phi^2} \mathbf{g} \int 4\pi dq q^2 \frac{1}{\sqrt{q^2 + a^2 m_0^2}} f(q) \sim \left(8.4 \times 10^{-5} \frac{g/m_\phi}{\text{eV}^{-1}} \right)^2, \quad (3.7)$$

where we have used $T_{\nu,0} = 0.1681$ meV and $\mathbf{g} = 6$ for the numerical estimate. Then, the equation of motion (2.15) simplifies to

$$\ddot{\phi} + M_\phi^2 \phi = 0, \quad (3.8)$$

which is the equation of a quadratic harmonic oscillator, with standard solution

$$\phi(a, t) = A(a) \sin(M_\phi t + \varphi_0), \quad (3.9)$$

with φ_0 an initial phase. In this case, it is trivial to average over an oscillation of the field, and for instance the total energy density is given by

$$\rho(a) = \frac{1}{2} M_\phi^2 A^2 + \rho_\nu(a, 0), \quad (3.10)$$

where $\rho_\nu(a, 0)$ is the energy density of neutrinos as if they were decoupled. The evolution of this energy density is compared to standard ν +ULDM in figure 3. While everything looks very similar, we can see that $\rho_\phi \equiv \frac{1}{2} \langle \dot{\phi}^2 \rangle + \frac{1}{2} m_\phi^2 \langle \phi^2 \rangle$ scales like radiation for $a < a_{\text{tr}}$.

The radiation behaviour of ρ_ϕ can be understood at the same time as one explains why a_{tr} also describes the transition between $A \sim a^{-3/2}$ and $A \sim a^{-1}$ from eq. (2.21). This stems from the conservation of the number of ϕ particles, i.e., the scaling of its number density as $n_\phi \sim a^{-3}$ [56]. Its energy density is, in turn, $\rho_\phi = M_\phi n_\phi$. For $a > a_{\text{tr}}$, M_ϕ is constant, and thus $\rho_\phi = m_\phi n_\phi \sim a^{-3}$. Since $\rho_\phi \equiv \frac{1}{2} m_\phi^2 A^2$, this means that $A \sim a^{-3/2}$, as standard CDM. However, when $a < a_{\text{tr}}$, $\rho_\phi = \delta m_\phi n_\phi \sim a^{-4}$, as if it were radiation. Since $\rho_\phi \equiv \frac{1}{2} \delta m_\phi^2 A^2$, this means that $A \sim a^{-1}$. Since ϕ is homogeneous, we expect perturbations to still behave as CDM with zero momentum, but the exact treatment of perturbations is left for future work. In order to better understand the effect of this transition in the expansion history of the Universe, we now quantitatively compute the equation of state.

3.2 Pressure and equation of state

From the energy-momentum tensor, the pressure of the fermion-pseudoscalar fluid is

$$p(a) = \frac{1}{2} \langle \dot{\phi}^2 \rangle - \frac{1}{2} m_\phi^2 \langle \phi^2 \rangle + \langle p_\nu(a, \phi) \rangle, \quad (3.11)$$

with

$$p_\nu(a, \phi) = \mathbf{g} \int d^3 \vec{p} \frac{p^2}{\sqrt{p^2 + m_0^2 + g^2 \phi^2}} f_0(pa) = a^{-4} \mathbf{g} \int \frac{4\pi dq q^4}{\sqrt{q^2 + a^2(m_0^2 + g^2 \phi^2)}} f_0(q). \quad (3.12)$$

In the linearised regime approximation, this can be simplified to

$$p(a, t) = \frac{1}{2} \dot{\phi}^2 - \frac{1}{2} m_\phi^2 \phi^2 - \frac{1}{2} \delta \mu_\phi^2 \phi^2 + p_\nu(a, 0), \quad (3.13)$$

where

$$\delta \mu_\phi^2 = -2 \left. \frac{\partial p_\nu(a, \phi)}{\partial \phi^2} \right|_{\phi=0} = a^{-2} g^2 \mathbf{g} \int 4\pi dq \frac{q^4}{(q^2 + a^2 m_0^2)^{3/2}} f_0(q) \quad (3.14)$$

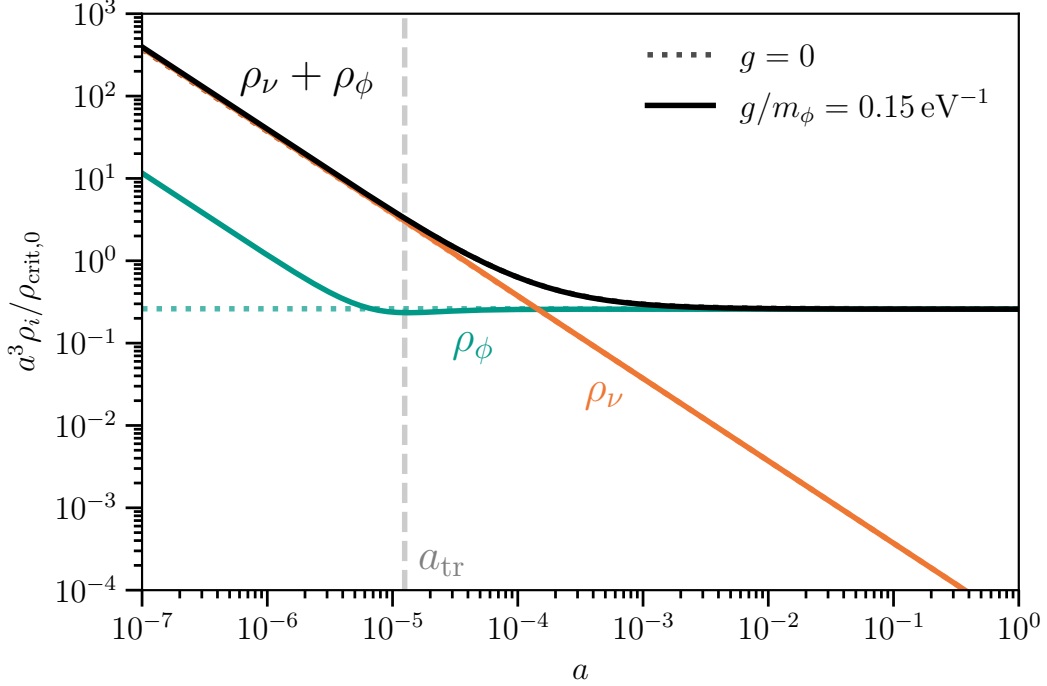


Figure 3. Evolution of the energy density of the ν +ULDM fluid, in the interacting scenario (solid) and in the decoupled scenario (dotted). In both cases, $m_0 = 10^{-5}$ eV. A vertical dashed line shows the time of transition between m_ϕ -domination and ν -domination. ρ_ϕ (teal) and ρ_ν (orange) can only be understood as independent fluids for $a \gg a_{\text{tr}}$. For $a < a_{\text{tr}}$, their separation is artificial.

is a higher-order integral of the momentum distribution. Now, plugging the solution from eq. (3.9) and averaging over an oscillation,

$$p(a) = \frac{1}{4} \left(\delta m_\phi^2 - \delta \mu_\phi^2 \right) A^2 + p_\nu(a, 0). \quad (3.15)$$

Since $\delta m_\phi^2 \geq \delta \mu_\phi^2$, the scalar part of the pressure is never negative. Then, one can define an equation of state for the total fluid,

$$w(a) = \frac{p(a)}{\rho(a)} = \frac{\left(\delta m_\phi^2 - \delta \mu_\phi^2 \right) A^2 / 4 + p_\nu(a, 0)}{\left(m_\phi^2 + \delta m_\phi^2 \right) A^2 / 2 + \rho_\nu(a, 0)}. \quad (3.16)$$

Now, we can simplify this expression further. In the early universe, for allowed values of m_0 , $T_\nu \gg m_0$, and m_0 can be neglected in integrals over the distribution function. In this limit, $\delta m_\phi^2 = \delta \mu_\phi^2$, and therefore

$$p(a) = p_\nu(a, 0) = \frac{1}{3} \rho_\nu(a, 0), \quad (3.17)$$

the pressure of the total fluid is only the pressure of the neutrino part, *as if they were uncoupled from the pseudoscalar field*, which are completely relativistic at early times. This simplifies the equation of state to

$$w(a) = \frac{1}{3} \frac{\rho_\nu(a, 0)}{\rho_\nu(a, 0) + \left(m_\phi^2 + \delta m_\phi^2 \right) A^2 / 2} = \frac{1}{3} \left[1 - \left(1 + \frac{\rho_\nu(a, 0)}{\left(m_\phi^2 + \delta m_\phi^2 \right) A^2 / 2} \right)^{-1} \right]. \quad (3.18)$$

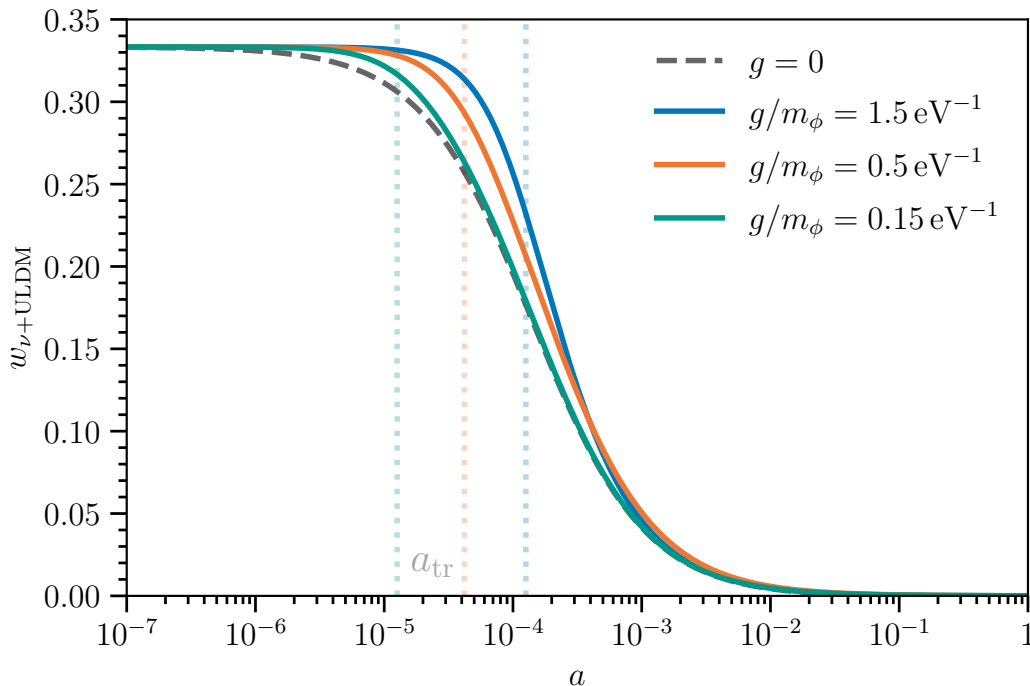


Figure 4. Evolution of the equation state of the ν +ULDM fluid for interacting scenarios (solid lines) and a decoupled scenario (dotted). Vertical dotted lines shows a_{tr} (transition between ν -domination and m_ϕ domination) for the different couplings, as in eq. (3.7). *The coupled fluid stays relativistic for a longer period.*

Figure 4 shows the evolution of $w(a)$ for different couplings. For the standard scenario $g \rightarrow 0$, $\delta m_\phi^2 = 0$. Then, if $m_\phi^2 A^2 \gg \rho_\nu(a, 0)$, $w = 0$ (CDM domination); and if $m_\phi^2 A^2 \ll \rho_\nu(a, 0)$, $w = 1/3$ (relativistic neutrino domination). In the coupled scenario, the modified scaling of $A(a)$ makes $w(a)$ grows faster to $1/3$ than in the standard case. One of the consequences of the fluid staying relativistic for a longer time is that the time of equality between matter and radiation is delayed [56]. However, for couplings allowed by BBN this is a subleading effect, as we will explore below.

3.3 Initial conditions

We want to impose that ϕ makes up all DM, namely $\Omega_{\phi,0} h^2 = \Omega_{c,0} h^2 = 0.1200$ [87], with $h = 0.6766$ the reduced Hubble constant. This requires that the amplitude of the field today is

$$A(a = 1) \equiv A_0 = \frac{\sqrt{2\Omega_{c,0} \rho_{\text{crit}}}}{m_\phi}, \quad (3.19)$$

assuming $m_\phi > \delta m_\phi$ today. The value of A today fixes the value of the adiabatic invariant $\mathcal{I}(a) = \mathcal{I}_0$, and allows to compute $A(a)$ at all times if we know $f_0(q)$. As proved in appendix A, the coupling with ϕ does not change the evolution of $f_0(q)$, and therefore its shape is frozen from its initial conditions, i.e., neutrino decoupling.

The early-Universe physics and, in particular, decoupling depend on the time of the misalignment mechanism. In standard ULDM, oscillations start when the potential energy term is larger than the Hubble friction, i.e., $m_\phi > 3H$. However, the interaction modifies

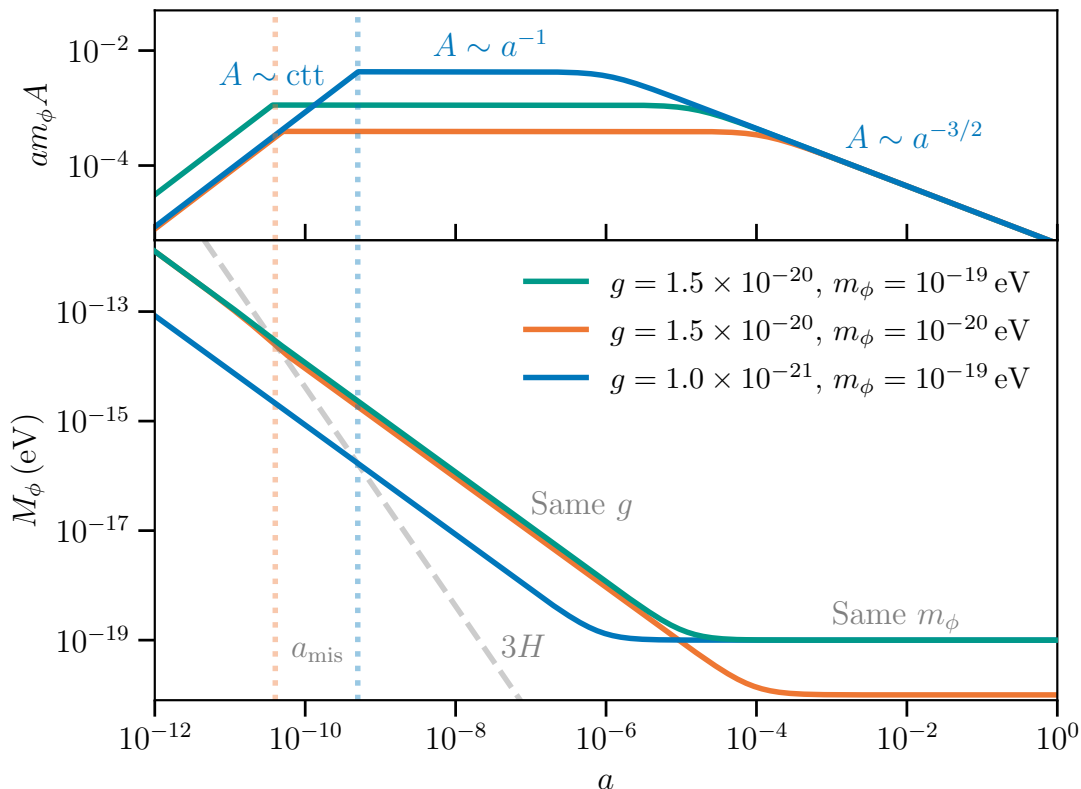


Figure 5. Effective mass M_ϕ , misalignment mechanism and evolution of the amplitude. From left to right, initially $3H > M_\phi$, and thus $A(a)$ remains constant. At misalignment, $3H \sim M_\phi$, the field starts evolving as a^{-1} if $a < a_{\text{tr}}$ or as $a^{-3/2}$ if $a > a_{\text{tr}}$. Curves with the same coupling g satisfy the misalignment condition at similar times, while fields with the same m_ϕ arrive at the same point in M_ϕ . Here, the amplitude today is set to match the abundance of DM, and thus $A_0 \sim m_\phi^{-1}$.

the condition to $M_\phi > 3H$. This advances misalignment, a_{mis} , to earlier times, as shown in figure 5.

Since $A_0 \propto m_\phi^{-1}$ and A always appears as gA , many of the cosmological observables depend only on g/m_ϕ . However, $\delta m_\phi^2 \sim g^2$ is independent of m_ϕ . Thus, the misalignment mechanism $3H < M_\phi$ breaks the degeneracy between g and m_ϕ . We find that, for couplings such that $\delta m_\phi^2 > m_\phi^2$, misalignment happens at

$$a_{\text{mis}} \simeq 10^{-11} \left(\frac{5 \times 10^{-20}}{g} \right). \quad (3.20)$$

Decoupling happens approximately at $T_\gamma \sim 2 \text{ MeV}$, which — assuming a naive linear scaling for temperature — corresponds to $a \sim 10^{-11}$. That is, misalignment happens after decoupling roughly if $g \lesssim 5 \times 10^{-20}$. Two scenarios open up,

- Before misalignment, m_ν is constant, T_ν/m_ν grows to the past and neutrinos are relativistic soon before misalignment. If misalignment happens after decoupling, $g \lesssim 5 \times 10^{-20}$, then neutrinos are relativistic at decoupling and effects from the interaction are negligible. If they are, their distribution function at later times will be a relativistic Fermi-Dirac such as eq. (2.14).

- If misalignment happens while neutrinos are in thermal equilibrium with the baryon plasma, $g \gtrsim 5 \times 10^{-20}$, then the growth of $A(a)$ might make them non-relativistic. Then, their distribution function will deviate from a Fermi-Dirac with m_ν/T_ν corrections. The full treatment requires thermal masses [60], but also to consider the effect of scatterings mediated by ϕ , far from the extent of this work.

With this in mind, we assume that misalignment happens after decoupling, and we approximate the misalignment to be instantaneous at $3H = M_\phi$. Before misalignment, we set $\phi = A$ and no oscillation is needed. At misalignment, ϕ starts to oscillate with M_ϕ and all observables are averaged as in eq. (2.16). This approximation produces an artificial discontinuity between unaveraged and averaged variables. A smooth misalignment should not strongly modify the results.

3.4 Massive neutrinos and N_{eff}

The neutrino-feedback into the pseudoscalar field has two main phenomenological consequences, an increased effective mass for neutrinos and an increase of early radiation.

Firstly, neutrinos will acquire a mass given by

$$\langle m_\nu \rangle = \langle m_\nu(\phi) \rangle = \left\langle \sqrt{m_0^2 + g^2 \phi^2} \right\rangle, \quad (3.21)$$

where the average is taken over the oscillation of the field. In the linearized regime, and for early enough in the Universe, $\langle m_\nu \rangle \simeq gA/\sqrt{2}$. Figure 6 compares the evolution of the neutrino mass and T_ν , which is related to the mean momentum of the distribution. While early enough, the neutrino mass can reach $\mathcal{O}(1)$ MeV, the important quantity is the *relativisticness* (i.e., velocity) of neutrinos, $T_\nu/\langle m_\nu \rangle$. That is, the interaction with the field can make them non-relativistic, $\langle m_\nu \rangle \gg T_\nu$. Figure 6 also shows how $T_\nu/\langle m_\nu \rangle$ diminishes as $a^{-1/2}$ for $a > a_{\text{tr}}$, while $T_\nu/\langle m_\nu \rangle$ becomes constant for $a < a_{\text{tr}}$. At misalignment, ϕ freezes and neutrinos become relativistic soon enough.

Secondly, if we fix the right DM abundance today, a longer radiation epoch as shown in figure 4 increases the amount of radiation in the early Universe, conventionally described by the number of relativistic degrees of freedom,

$$N_{\text{eff}} = \frac{\rho_{\text{rad}} - \rho_\gamma}{\frac{7}{8} \left(\frac{4}{11}\right)^{4/3} \rho_\gamma}, \quad (3.22)$$

where ρ_{rad} , ρ_γ are the energy densities for all radiation and photons, respectively. We quantify the contribution of our model with $\Delta N_{\text{eff}} = N_{\text{eff}} - 3.044$. Figure 7 shows the evolution of ΔN_{eff} in our model. The radiation excess is specially significant at the pre-CMB epoch, as expected from eq. (3.7). As a consequence, we expect BBN to put better constraints on the neutrino feedback of the model. Figure 7 also shows a short depletion of N_{eff} at the time of misalignment, which is an artifact of the instantaneous misalignment approximation. Namely, since at $a < a_{\text{mis}}$ we set $\phi = A$ and skip oscillations, then $m_\nu = gA$ instead of $\langle m_\nu \rangle = gA/\sqrt{2}$, neutrinos become slightly non-relativistic and decrease ρ_{rad} . However, as soon as the plasma heats the constant mass of neutrinos becomes negligible, thus making them relativistic and retrieving $\Delta N_{\text{eff}} = 0$.

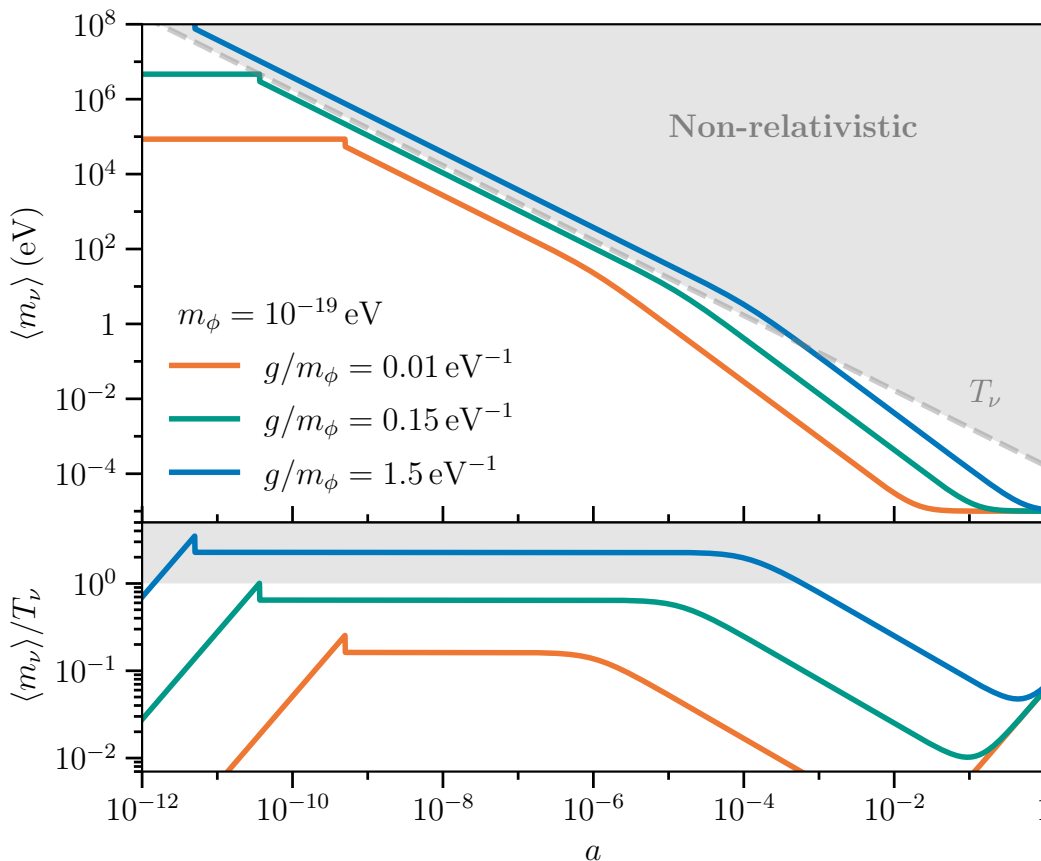


Figure 6. Evolution of average neutrino mass, $\langle m_\nu \rangle$, and its *non-relativisticness*, i.e., $\langle m_\nu \rangle / T_\nu$. Initially, $m_\nu \sim m_0 = 10^{-5}$ eV, and soon $\langle m_\nu \rangle \sim gA/\sqrt{2}$. Thus, $\langle m_\nu \rangle$ follows $A(a)$, shown in figure 5. For large (excluded) couplings, neutrinos become non-relativistic. Since the linearised approximation is an expansion on $(\langle m_\nu \rangle / T_\nu)^2$, the bottom plot justifies the validity of the approximation for non-excluded couplings.

4 Big Bang Nucleosynthesis

Big Bang Nucleosynthesis (BBN) is the process by which the primordial light elements are formed in the first twenty minutes of the Universe, from the reactions between protons (p), neutrons (n), electrons, and electron neutrinos. The abundances of the primordial light elements are measured by astrophysical observations. Helium-4 and deuterium abundances are the best understood and have been measured to be [88, 89]

$$\begin{aligned} Y_{\text{P}} &\equiv X_{4\text{He}} = 0.245 \pm 0.003, \\ \text{D}/\text{H} &\equiv n_{\text{D}}/n_{1\text{H}} = (2.547 \pm 0.025) \times 10^{-5}, \end{aligned} \tag{4.1}$$

respectively. A joint fit with the CMB provides an excellent agreement between the two cosmological probes, and the excellent agreement with the SM makes BBN a powerful probe of BSM physics in the very-early Universe. In this section, we implement our model in the full calculation of BBN abundances and constrain the model from there.

The impact of the model in BBN is two-fold. First, ΔN_{eff} will increase the Hubble rate, thus making nuclear processes less efficient and modifying the duration of nucleosynthe-

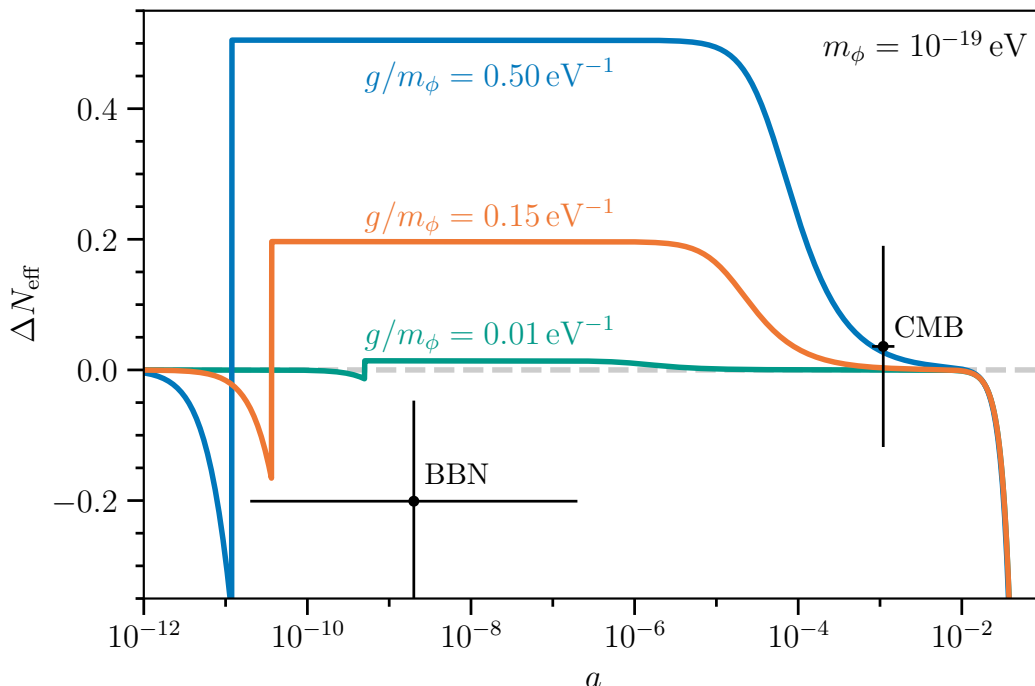


Figure 7. Number of relativistic neutrino species for different values of the coupling. The dilation of the radiation phase, shown in figure 4, increases the amount of radiation in the early universe. Data points show the measurements of N_{eff} at CMB and BBN, with horizontal errorbars showing the approximate duration of each epoch. Couplings which have a significant impact on BBN are negligible at CMB. *BBN is the best epoch to constrain this model.*

sis. Secondly, the non-zero mass of neutrinos will modify the kinematics of the reactions and thus the interaction rates Γ . For instance, if neutrinos had mass $m_\nu > \Delta - m_e$, with $\Delta = m_n - m_p \simeq 1.29333 \text{ MeV}$, neutron decay would be forbidden, greatly increasing Y_p .

In order to implement neutrino masses in $n \rightarrow p$ (and viceversa) interaction rates, we follow the Born approximation, where neutrons and protons are approximated to have infinite mass. In this limit, interaction rates from all processes are given by [90],

$$\begin{aligned} \Gamma_{n \rightarrow p} &= \tilde{G}_F^2 \int_0^\infty dE_e E_e E_\nu^- \sqrt{E_e^2 - m_e^2} \sqrt{E_\nu^- - m_\nu^2} [f_\nu(E_\nu^-) f_e(-E_e) + f_\nu(-E_\nu^-) f_e(E_e)], \\ \Gamma_{p \rightarrow n} &= \tilde{G}_F^2 \int_0^\infty dE_e E_e E_\nu^+ \sqrt{E_e^2 - m_e^2} \sqrt{E_\nu^+ - m_\nu^2} [f_\nu(E_\nu^+) f_e(-E_e) + f_\nu(-E_\nu^+) f_e(E_e)]. \end{aligned} \quad (4.2)$$

Here, $\tilde{G}_F^2 = G_F V_{\text{ud}} \sqrt{(1 + 3g_A^2)/(2\pi^3)}$ with G_F the Fermi constant, V_{ud} the Cabibbo angle and g_A the axial electroweak coupling; and $E_\nu^\pm = E_e \pm \Delta$. The distribution functions f_ν , f_e follow Fermi-Dirac distributions as in eq. (2.14), controlled by T_ν and T_γ , respectively. These implement the amount of allowed fermions for the interaction if in the initial state, or Pauli blocking if in the final state. These rates are shown in figure 8.

Now, $\Gamma = \Gamma(\phi)$ through $m_\nu = m_\nu(\phi)$. Before misalignment, $3H > M_\phi$, the field is frozen and oscillations need not be taken into account. However, after misalignment, the field oscillates and Γ needs to be averaged. Different timescales play a role here. First, the

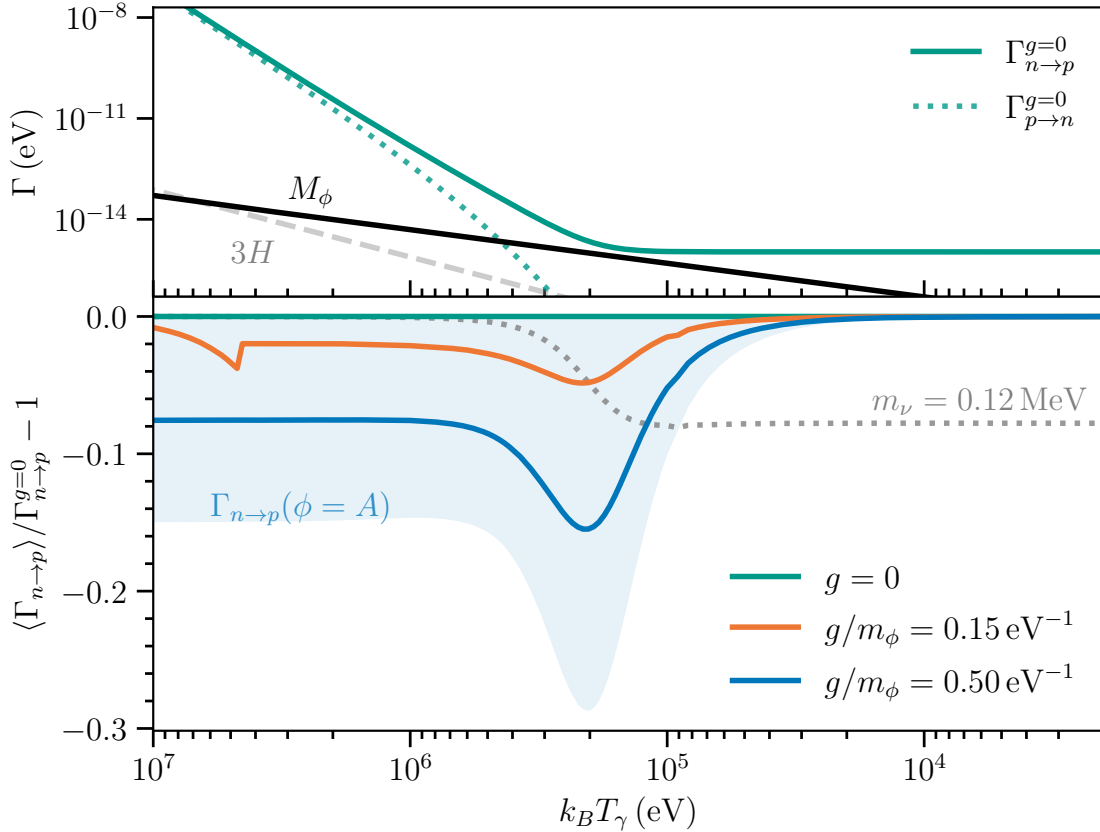


Figure 8. Neutron-to-proton (and viceversa) interaction rates $\Gamma_{n \rightarrow p}$ ($\Gamma_{p \rightarrow n}$) at the temperatures relevant for BBN, and the effect of ν -ULDM interactions in them. In the top plot, we compare Γ to the other relevant timescales of the problem, and check that $3H > \Gamma, M_\phi$; which requires us to average over ϕ oscillations, as described in the main text. M_ϕ is shown for $g/m_\phi = 0.15 \text{ eV}^{-1}$. In the bottom plot, we see how the coupling reduces the $n \rightarrow p$ interaction rate. For comparison, we show the effect of a constant mass $m_\nu = 0.12 \text{ MeV}$ (dotted line). The blue shaded region encloses $\Gamma_{n \rightarrow p}(\phi)$ for all possible values of $\phi < A(a)$. Thus, the solid blue line is the average of the blue shaded region. A larger neutrino mass decreases the interaction rate, which will increase the helium and deuterium abundances.

oscillation of the field is always much slower than the timescale of the electroweak vertex, $M_\phi^2 \ll G_F^{-1}$, and therefore electroweak interactions happen within a constant value of the field. Then, two regimes can follow,

- If $\Gamma > M_\phi$, many interactions happen within an oscillation of the field, and so eq. (4.2) can reach equilibrium within a constant m_ν . Since ϕ oscillates many times within cosmological timescales, we need to average Γ over each $m_\nu(\phi)$.
- If $\Gamma < M_\phi$, interactions happen only once every many oscillations. At cosmological scale, with $\Gamma > H$, still many interactions happen, each of them effectively at a random value of $m_\nu(\phi)$. Then, the result is still an effective averaged Γ .

In any case, we must average as in eq. (2.16)

$$\langle \Gamma \rangle = t_\phi^{-1} \oint \frac{\Gamma(\phi)}{\dot{\phi}} d\phi, \quad (4.3)$$

where $\Gamma(\phi)$ is given by eq. (4.2) with $m_\nu = m_\nu(\phi)$. Finally, neutrinos do not play a role in the subsequent thermonuclear interactions, and therefore hadronic rate are unmodified by non-zero m_ν . We implement the modified expansion history and expansion rates from eqs. (4.2) and (4.3) in the numerical code `PRyMordial` [90]. Figure 8 shows how the coupling reduces $\langle \Gamma_{n \rightarrow p} \rangle$. As a consequence, a reduced $n \rightarrow p$ interaction rate will then increase Y_P .

5 Results and discussion

The modified version of `PRyMordial` allows to compute all the light element abundances. From all the observed abundances, we discard ^3He , for which only an upper limit exists, and ^7Li , which is currently anomalous. Thus, restricting the analysis to the abundances given in eq. (4.1) makes it more conservative and robust. Figure 9 shows how an increased interaction rate increases the expected abundances, far above the observed values. The results also indicate that, while both ΔN_{eff} and m_ν increase the final abundances, the Y_P result is more sensitive to m_ν than to ΔN_{eff} and is the dominant quantity driving the constraints. Black crosses show the expected $g \rightarrow 0$ limit of the full BBN computation, beyond the Born approximation and including next-to-leading order (NLO) corrections. Computation of these corrections in this model is beyond the scope of our work. However, the $g \rightarrow 0$ limit shown in figure 9 hints that NLO corrections also increase the final abundances, and in this case our bounds can be understood as conservative.

Then, for every point in the (g, m_ϕ) parameter space we can define a χ^2 function,

$$\chi^2(g, m_\phi) = \left(\frac{Y_P(g, m_\phi) - Y_P^{\text{obs}}}{\sigma_{Y_P}} \right)^2 + \left(\frac{(D/H)(g, m_\phi) - (D/H)^{\text{obs}}}{\sigma_{D/H}} \right)^2, \quad (5.1)$$

where Y_P^{obs} ($(D/H)^{\text{obs}}$) is the observed value of the ^4He (^2H) abundance, and σ_{Y_P} ($\sigma_{D/H}$) its 1σ uncertainty, as given in eq. (4.1). We perform a hypothesis test by defining

$$\Delta\chi^2 \equiv \chi^2(g, m_\phi) - \chi^2(g = 0), \quad (5.2)$$

where $\chi^2(g = 0)$ is the value of eq. (5.1) at $g = 0$, i.e., the null hypothesis. The 95% C.L. contours of this function is presented in figure 10. At $m_\phi \gtrsim 3 \times 10^{-20} \text{ eV}$, the bound is $g \lesssim 0.13(m_\phi/\text{eV})$. At this region, misalignment happens before BBN, and all observable effects depend only on g/m_ϕ . However, as explained in section 3.3, bounds for $g \gtrsim 5 \times 10^{-20}$ (region hatched with crosses) depend on the physics of decoupling and might be corrected by thermal effects [59, 60]. At $m_\phi \lesssim 3 \times 10^{-20} \text{ eV}$, misalignment happens at some point in BBN. Previous to misalignment, the feedback effects disappear and BBN loses constraining power, thus weakening the bound to $g \lesssim 1.8 \times 10^{-11} \sqrt{m_\phi/\text{eV}}$. Finally, a region hatched with circles shows where neutrino self-interactions mediated by ϕ are relevant for a scalar coupling. Since our bound is below this region, our bound also applies to the scalar coupling.

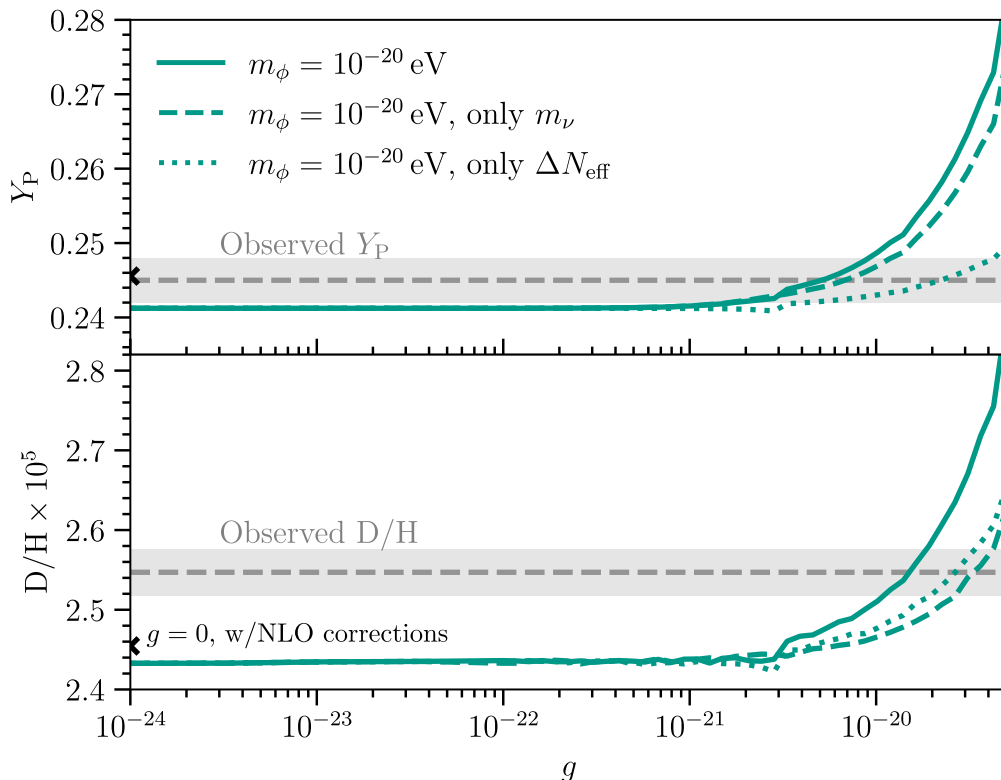


Figure 9. Prediction on primordial abundances of ${}^4\text{He}$ and deuterium for different values g , at $m_\phi = 10^{-19}$ eV. Solid lines show the prediction including all effects of our model, while a dotted line includes only the modification of neutrino masses (i.e., $\Delta N_{\text{eff}} = 0$ artificially), and a dashed line only the modification of N_{eff} (i.e., $m_\nu = 0$). A black cross shows the results at $g = 0$ beyond the Born approximation, including next-to-leading order contributions, and a grey band shows the 1σ contours of the observed values [89].

Due to the Milky Way DM halo, the local DM density is larger than the cosmological mean field value that we have defined up to now. In particular, $\rho_{\text{DM}}^\odot = 0.3 \text{ GeV cm}^{-3}$. Taking this into account, it would be specially interesting if this model could predict the right order of magnitude for neutrino masses without requiring the extra parameter m_0 . Neglecting m_0 , this means

$$\langle m_\nu^\odot \rangle \simeq \frac{g}{m_\phi} \sqrt{\rho_{\text{DM}}^\odot} = 2 \times 10^{-4} \left(\frac{g/m_\phi}{0.13 \text{ eV}^{-1}} \right) \text{ eV}. \quad (5.3)$$

Setting the target neutrino mass to $m_\nu^\odot \sim \sqrt{|\Delta m_{3\ell}^2|} = 3 \times 10^{-3}$ eV, in the mass range studied here this would only be reached at couplings saturating the bound for $m_\phi \sim 10^{-22}$ eV.

6 Conclusions and outlook

The nature of DM and the origin of neutrino masses are two yet unsolved mysteries of particle physics. Models which connect both of these sectors are theoretically motivated and phenomenologically rich. In particular, models of ULDM are gaining interest in the community. In this article, we have explored the phenomenological implications of a coupling

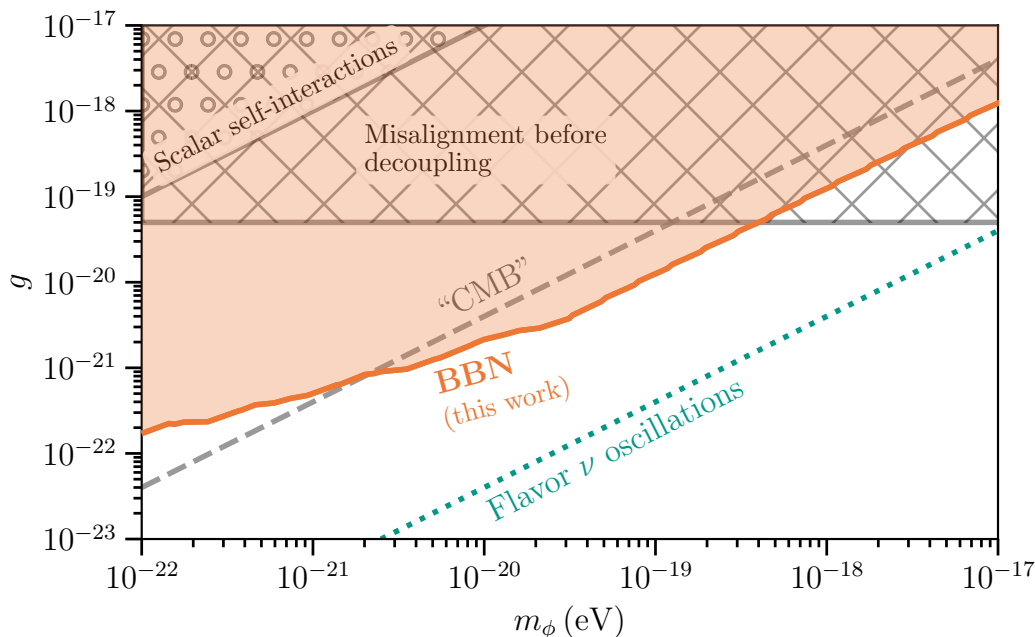


Figure 10. 95% C.L. exclusion regions for the $\nu - \phi$ coupling (as defined in eq. (2.1)), for the test statistic defined in eq. (5.2). A gray dashed line shows the bound for a scalar coupling to RHNs, from CMB [56]. A green dotted line shows a bound for this same model, assuming it has flavor structure and gives rise to time-dependent neutrino oscillations [35]. The region hatched with crosses corresponds to misalignment happening before neutrino decoupling, meaning neutrinos can be non-relativistic at decoupling and modify their distribution function from the here-assumed Fermi-Dirac. The region with circles shows where neutrino self-interactions mediated by a scalar ϕ are relevant.

between ULDM and the neutrino sector in the early Universe. As a result, we have presented a quantitative bound from a full cosmological evolution of such models.

In this work we have quantitatively solved the equations of motion for the ULDM field, which have a large separation of scales between the frequency of ϕ oscillations and cosmological evolution. To such purpose, we follow an adiabatic approximation which provides an invariant quantity with which to compute the amplitude of the field at every time. This method predicts that the scaling of the ULDM field changes when the neutrino interaction potential dominates over its mass potential, from $a^{-3/2}$ to a^{-1} .

Two observable consequences in the early Universe derive from this scaling transition. First, neutrino masses scale linearly with the scale factor, and thus their velocity, related to T_ν/m_ν , stays constant. This is shown in figure 6. When compared to the naive scaling of $a^{-3/2}$, this weakens the effect of time-dependent neutrino masses in the early Universe. Second, the modified scaling also reduces the contribution of the bare-mass potential, $m_\phi^2\phi^2$, to the total energy of the system. As a consequence, the coupled ν -ULDM stays relativistic for a longer time, as in figure 4. If then we ask for ϕ to fulfill the totality of DM, this requires that the radiation energy density in the early Universe is slightly larger, which contributes positively to N_{eff} , as in figure 7.

Finally, we implement this two phenomenological consequences in Big Bang Nucleosynthesis using the PRyMordial code [90]. We modify the $n \rightarrow p$ and $p \rightarrow n$ interaction rates

to account for a non-zero neutrino mass, following the Born approximation. Since these rates are faster than the oscillation frequencies and the cosmological evolution, we average them for the oscillation of the ULDM field. Using the modified rates and N_{eff} , we compute the primordial element abundances for different (g, m_ϕ) , as in figure 9. Comparing these to observations, we present our bounds on the parameter space of the model in figure 10, which improve CMB bounds by a factor ~ 4 .

The non-trivial dynamics of the coupled fluid are an unexpected consequence of ν -ULDM which open new research possibilities. In particular, in this work we have focused on BBN consequences since we *a priori* expect it to provide stronger constraints on the model. Still, two arguments motivate using the CMB to further understand and constrain this model. First, the dynamics of ν -ULDM cosmological perturbations could produce unexpected leading-order effects. Second, a joint CMB+BBN analysis would simultaneously infer Ω_b , g , and m_ϕ , potentially modifying constraints by breaking degeneracies between these parameters. However, standard CMB analyses assume that N_{eff} is consistent between BBN and CMB epochs. As figure 7 shows, this is not the case here. This discrepancy motivates a more refined analysis where the relationship between Y_p and $N_{\text{eff}}(a_{\text{CMB}})$ is adjusted for the model.

The coupling that we have used should be understood as a first approach to ν -ULDM couplings with time-varying masses. Other couplings, which have more theoretically motivated SM extensions, have been proposed in the literature. Even if their phenomenological implications have already been explored [56, 59], it would be interesting to extend the quantitative analysis here presented into such models to place consistent bounds into them.

All in all, cosmology remains an exciting framework within which to look for signatures of BSM particle physics models, specially for particles which interact extremely feebly. That is, the large particle number densities involved compensate for the small couplings. This is specially interesting for interactions which involve the neutrino sector. At the same time, cosmology is a complex science with a lot of subtleties that must be under control in order to produce robust statements. In this work we have tried to clarify some of such details and to make claims on ν -ULDM claims consistent and quantitative.

Acknowledgments

The authors thank Iván Esteban and Concha González-García for early discussions on neutrino self interactions, and Anne-Katherine Burns for help on the use of `PRyMordial` and BBN. This work has been supported by the Spanish MCIN/AEI/10.13039/501100011033 grants PID2022-126224NB-C21 and by the European Union’s Horizon 2020 research and innovation program under the Marie Skłodowska-Curie grants HORIZON-MSCA-2021-SE-01/101086085-ASYMMETRY and H2020-MSCA-ITN-2019/860881-HIDDeN, and by the “Unit of Excellence Maria de Maeztu 2020-2023” award to the ICC-UB CEX2019-000918-M (TB and JS). TB is supported by the Spanish grant PRE2020-091896. JLS is supported by Grants PGC2022-126078NB-C21 funded by MCIN/AEI/10.13039/501100011033 and “ERDF A way of making Europe” and Grant DGA-FSE grant 2020-E21-17R Aragon Government and the European Union-NextGenerationEU Recovery and Resilience Program on “Astrofísica y Física de Altas Energías” CEFCA-CAPA-ITAINNOVA.

A Details on the formalism

In this appendix, we formalize definitions for variables and functions defined in the main text.

A.1 Solutions to the equations of motion

Firstly, eq. (2.4) introduces the classical expectation value for a certain quantum operator $\hat{\mathcal{O}}$,

$$\langle \hat{\mathcal{O}} \rangle = \sum_s \int dP_1 dP_2 dP_3 \frac{1}{\sqrt{-\det g}} \frac{1}{2P^0} f(P, x, s) \langle \phi, P^s | \hat{\mathcal{O}} | \phi, P^s \rangle. \quad (\text{A.1})$$

Here, $|\phi, P^s\rangle = |\phi\rangle \otimes |P^s\rangle$ is the product of a coherent state with field ϕ and a one-particle fermion state, given by [91–94]

$$\begin{aligned} |\phi\rangle &\equiv \exp \left\{ -\frac{1}{2} \int \frac{d^3 \vec{k}}{(2\pi)^3} \frac{|\phi(K)|^2}{(2K^0)^5} \right\} \exp \left\{ \int \frac{d^3 \vec{k}}{(2\pi)^3} \frac{\phi(K)}{(2K^0)^{5/2}} a_K^\dagger \right\} |0\rangle, \\ |P^s\rangle &= \sqrt{2P^0} a_P^{s\dagger} |0\rangle. \end{aligned} \quad (\text{A.2})$$

Here, $|0\rangle$ is the vacuum state, a_P^s (a_K^ϕ) is the annihilation operator of the field ψ (ϕ), $K^\mu = (E_K, \vec{k})$ such that $K^2 = -m_\phi^2$, and $\phi(K)$ is the Fourier transform of the classical scalar field $\phi(x)$,

$$\phi(x) \equiv \int \frac{d^3 \vec{k}}{(2\pi)^3} \frac{1}{(\sqrt{2}K^0)^3} \left[\phi(K) e^{-iKx} + \phi(K)^* e^{iKx} \right]. \quad (\text{A.3})$$

Then, P_μ is the conjugate momentum to x^μ , and is related to the 4-momentum of the particle P^ν by $P_\mu = g_{\mu\nu} P^\nu$, and to the physical momentum $p^i = p_i$ as $P_i = ap_i$. The 4-momentum of the particle is described by the geodesic equation

$$P^0 \frac{dP^\mu}{d\eta} + \Gamma^\mu_{\nu\rho} P^\nu P^\rho = 0. \quad (\text{A.4})$$

In a homogeneous Universe, this returns that the physical linear momentum, $p_i = P_i/a$, decreases as a^{-1} as the Universe expands. In this work, we have worked with the comoving linear momentum, $q_i = ap_i$, which we describe in terms of its magnitude and direction, $q_i = qn_i$.

The general solution to the Dirac equation, eq. (2.3), is

$$\psi = \int \frac{d^3 \vec{p}}{(2\pi)^3} \frac{1}{\sqrt{2E_p}} \sum_{s=1,2} \left(e^{-iPx} a^s(\vec{p}) u^s(\vec{p}) + e^{iPx} b^{s\dagger}(\vec{p}) v^s(\vec{p}) \right), \quad (\text{A.5})$$

with

$$u^s(\vec{p}) = e^{i\alpha\gamma^5} u_0^s(\vec{p}), \quad v^s(\vec{p}) = e^{i\alpha\gamma^5} v_0^s(\vec{p}), \quad (\text{A.6})$$

the plane wave solutions, $P^\mu = (E_p, \vec{p})$ and $a^s(P)$ and $b^s(P)$ are the annihilation operators to $u^s(\vec{p})$ and $v^s(\vec{p})$. For instance, one can use the Pauli-Dirac representation of the gamma matrices,

$$\gamma^0 = \begin{pmatrix} \mathbb{I}_2 & 0 \\ 0 & -\mathbb{I}_2 \end{pmatrix}, \quad \gamma^i = \begin{pmatrix} 0 & \sigma^i \\ -\sigma^i & 0 \end{pmatrix}, \quad \gamma^5 = \begin{pmatrix} 0 & \mathbb{I}_2 \\ \mathbb{I}_2 & 0 \end{pmatrix}, \quad (\text{A.7})$$

with \mathbb{I}_2 the 2x2 identity matrix, and σ^i the Pauli matrices. Then, the positive and negative frequency solutions to eq. (2.8), with defined mass m_ν , are [95]

$$u_0^s(\vec{p}) = \begin{pmatrix} \sqrt{E_p + m_\nu} \xi^s \\ \frac{\vec{\sigma} \cdot \vec{p}}{\sqrt{E_p + m_\nu}} \xi^s \end{pmatrix}, \quad v_0^s(\vec{p}) = \begin{pmatrix} \frac{\vec{\sigma} \cdot \vec{p}}{\sqrt{E_p + m_\nu}} \chi^s \\ \sqrt{E_p + m_\nu} \chi^s \end{pmatrix}, \quad (\text{A.8})$$

respectively. Here $E_p = \sqrt{\vec{p}^2 + m_0^2 + g^2 \phi^2}$, and ξ^s, χ^s are spinors corresponding to the eigenvectors of a Stern-Gerlach experiment in an arbitrary \hat{n} direction, with $s = 1, 2$ that differentiates between the two helicity eigenstates. These must fulfill $\xi^{s\dagger} \xi^s = \chi^{s\dagger} \chi^s = 1$. With all this information, one can check that the plane wave solutions fulfill

$$\begin{aligned} \bar{u}^s(\vec{p}) \gamma^0 u^r(\vec{p}) &= \bar{v}^s(\vec{p}) \gamma^0 v^r(\vec{p}) = 2E \delta^{sr}, \\ \bar{u}^s(\vec{p}) \gamma^5 u^r(\vec{p}) &= -\bar{v}^s(\vec{p}) \gamma^5 v^r(\vec{p}) = 2ig\phi \delta^{sr}. \end{aligned} \quad (\text{A.9})$$

A.2 Evolution of the distribution function

In general, the neutrino phase space distribution $f(x^i, q, n_j, \eta)$ evolves according to the Boltzmann equation

$$\frac{Df}{d\eta} = \frac{\partial f}{\partial \eta} + \frac{dx^i}{d\eta} \frac{\partial f}{\partial x^i} + \frac{dq}{d\eta} \frac{\partial f}{\partial q} + \frac{dn_i}{d\eta} \frac{\partial f}{\partial n_i} = \frac{\partial f}{\partial \eta} \Big|_C. \quad (\text{A.10})$$

Here, the right-hand side describes the changes on the distribution function due to collisions. For a decoupled ($g = 0$) species with constant mass in a homogeneous Universe, $dq/d\eta = 0$, $dn_i/d\eta = 0$ and $\partial f/\partial x^i = 0$, which leads to $\partial f/\partial \eta = 0$. This means that any distribution function which depends on $q = pa$ is a solution to the homogeneous collisionless Boltzmann equation. That is, $f(x^i, P_j, \eta) = f_0(q)$, which will maintain its shape and only have the physical momenta redshifted by $p = q/a$.

However, our model includes mass-varying neutrinos with $m_\nu(\eta) = \sqrt{m_0^2 + g^2 \phi(\eta)^2}$, which might make us wonder if $dq/d\eta = 0$ as we had assumed in the standard case. To first order, we would then have

$$\frac{\partial f_0}{\partial \eta} + \frac{dq}{d\eta} \frac{\partial f_0}{\partial q} = 0, \quad (\text{A.11})$$

which could make $f_0(q)$ vary with time. However, for mass-varying neutrinos, the geodesic equation gets modified to [96]

$$P^0 \frac{dP^\mu}{d\eta} + \Gamma^\mu_{\nu\rho} P^\nu P^\rho = -m_\nu^2 \frac{d \log m_\nu}{d\phi} \frac{\partial \phi}{\partial x_\mu}. \quad (\text{A.12})$$

After some algebra, in the 0th component of the geodesic equation the contribution from ϕ vanishes and we still get

$$\frac{dq}{d\eta} = 0. \quad (\text{A.13})$$

Therefore, $\partial f_0/\partial \eta = 0$ and the shape of the momentum distribution function $f_0(q)$ does not vary with time, even for the mass-varying neutrinos from this model.

A.3 Derivation of the adiabatic invariant

Section 2.3 introduced the adiabatic approximation and obtained the adiabatic invariant $\mathcal{I}(a)$. In this section we describe the computations to arrive to this result.

We are interested in obtaining the evolution equation for ρ . To do so, we begin by multiplying eq. (2.13) by $\dot{\phi}$, and rewriting it into

$$\frac{d\rho(a, t)}{dt} = H \left[\frac{\partial \rho_\nu}{\partial \log a} - 3\dot{\phi}^2 \right]. \quad (\text{A.14})$$

Within cosmological timescales, the energy density varies as

$$H \frac{d\rho(a, t)}{d \log a} = \frac{d\rho(a, t)}{dt}. \quad (\text{A.15})$$

In the adiabatic approximation, we replace $d\rho/dt$ by its averaged value over an oscillation of the field

$$H \frac{d\rho}{d \log a} = \left\langle \frac{d\rho}{dt} \right\rangle. \quad (\text{A.16})$$

Now, plugging eq. (A.14) here,

$$\frac{d\rho}{d \log a} = \left\langle \frac{\partial \rho_\nu}{\partial \log a} \right\rangle - 3\langle \dot{\phi}^2 \rangle. \quad (\text{A.17})$$

Within an oscillation we can treat the total energy as a constant of motion, $\rho(a, t) \simeq \langle \rho(a, t) \rangle \equiv \rho(a)$. This allows to use eq. (2.18) to find a closed expression for $\dot{\phi}$,

$$\dot{\phi} = \sqrt{2} \sqrt{\rho(a) - m_\phi^2 \phi^2 / 2 - \rho_\nu(\phi)} \quad (\text{A.18})$$

Then,

$$t_\phi \langle \dot{\phi}^2 \rangle = \oint d\phi \dot{\phi} = \sqrt{2} \oint d\phi \sqrt{\rho(a) - \frac{1}{2} m_\phi^2 \phi^2 - \rho_\nu(\phi)}. \quad (\text{A.19})$$

This is an important quantity, since we notice that

$$\begin{aligned} t_\phi \frac{d\rho}{d \log a} - t_\phi \left\langle \frac{\partial \rho_\nu}{\partial \log a} \right\rangle &= \frac{1}{\sqrt{2}} \oint d\phi \frac{\partial(\rho(a) - \rho_\nu(a, \phi)) / \partial \log a}{\sqrt{\rho(a) - \frac{1}{2} m_\phi^2 \phi^2 - \rho_\nu(\phi)}} \\ &= \sqrt{2} \frac{d}{d \log a} \oint d\phi \sqrt{\rho(a) - \frac{1}{2} m_\phi^2 \phi^2 - \rho_\nu(\phi)} \\ &= \frac{d}{d \log a} (t_\phi \langle \dot{\phi}^2 \rangle). \end{aligned} \quad (\text{A.20})$$

Plugging this result into eq. (A.17), we get that

$$\frac{d}{d \log a} (t_\phi \langle \dot{\phi}^2 \rangle) = -3 t_\phi \langle \dot{\phi}^2 \rangle. \quad (\text{A.21})$$

So,

$$\mathcal{I}(a) \equiv \frac{1}{\sqrt{2}} a^3 t_\phi \langle \dot{\phi}^2 \rangle = a^3 \oint d\phi \sqrt{\rho(a) - \frac{1}{2} m_\phi^2 \phi^2 - \rho_\nu(\phi)} \quad (\text{A.22})$$

is an invariant quantity for the whole cosmological evolution, since $d\mathcal{I}/da = 0$. This adiabatic invariant allows to compute the total energy density $\rho(a)$ of the system as a function of the scale factor, given some initial conditions.

References

- [1] M. Cirelli, A. Strumia and J. Zupan, *Dark Matter*, [arXiv:2406.01705](#) [INSPIRE].
- [2] C.A.J. O’Hare, *Cosmology of axion dark matter*, *PoS COSMICWISPers* (2024) 040 [[arXiv:2403.17697](#)] [INSPIRE].
- [3] G. Arcadi et al., *The Waning of the WIMP: Endgame?*, *Eur. Phys. J. C* **85** (2025) 152 [[arXiv:2403.15860](#)] [INSPIRE].
- [4] M. Fabbrichesi, E. Gabrielli and G. Lanfranchi, *The Dark Photon*, [arXiv:2005.01515](#) [[DOI:10.1007/978-3-030-62519-1](#)] [INSPIRE].
- [5] Z.-J. Tao, *Radiative seesaw mechanism at weak scale*, *Phys. Rev. D* **54** (1996) 5693 [[hep-ph/9603309](#)] [INSPIRE].
- [6] E. Ma, *Verifiable radiative seesaw mechanism of neutrino mass and dark matter*, *Phys. Rev. D* **73** (2006) 077301 [[hep-ph/0601225](#)] [INSPIRE].
- [7] C. O’Hare, *cajohare/AxionLimits: AxionLimits*, [DOI:10.5281/zenodo.3932430](#).
- [8] P. Svrcek and E. Witten, *Axions In String Theory*, *JHEP* **06** (2006) 051 [[hep-th/0605206](#)] [INSPIRE].
- [9] M.B. Green, J.H. Schwarz and E. Witten, *Superstring theory. Vol. 2: loop amplitudes, anomalies and phenomenology*, Cambridge University Press, Cambridge, U.K. (1988).
- [10] A. Arvanitaki et al., *String Axiverse*, *Phys. Rev. D* **81** (2010) 123530 [[arXiv:0905.4720](#)] [INSPIRE].
- [11] M. Dine, *Supersymmetry and String Theory: Beyond the Standard Model*, Oxford University Press (2016) [[DOI:10.1017/9781009290883](#)] [INSPIRE].
- [12] J. Halverson, C. Long and P. Nath, *Ultralight axion in supersymmetry and strings and cosmology at small scales*, *Phys. Rev. D* **96** (2017) 056025 [[arXiv:1703.07779](#)] [INSPIRE].
- [13] T.C. Bachlechner, K. Eckerle, O. Janssen and M. Kleban, *Axion Landscape Cosmology*, *JCAP* **09** (2019) 062 [[arXiv:1810.02822](#)] [INSPIRE].
- [14] R. Essig et al., *Working Group Report: New Light Weakly Coupled Particles*, in the proceedings of the *Snowmass 2013: Snowmass on the Mississippi*, Minneapolis, U.S.A., July 29 – August 06 (2013) [[arXiv:1311.0029](#)] [INSPIRE].
- [15] J. Preskill, M.B. Wise and F. Wilczek, *Cosmology of the Invisible Axion*, *Phys. Lett. B* **120** (1983) 127 [INSPIRE].
- [16] L.F. Abbott and P. Sikivie, *A Cosmological Bound on the Invisible Axion*, *Phys. Lett. B* **120** (1983) 133 [INSPIRE].
- [17] M. Dine and W. Fischler, *The Not So Harmless Axion*, *Phys. Lett. B* **120** (1983) 137 [INSPIRE].
- [18] M.S. Turner, *Coherent Scalar Field Oscillations in an Expanding Universe*, *Phys. Rev. D* **28** (1983) 1243 [INSPIRE].
- [19] L. Hui, J.P. Ostriker, S. Tremaine and E. Witten, *Ultralight scalars as cosmological dark matter*, *Phys. Rev. D* **95** (2017) 043541 [[arXiv:1610.08297](#)] [INSPIRE].
- [20] L. Hui, *Wave Dark Matter*, *Ann. Rev. Astron. Astrophys.* **59** (2021) 247 [[arXiv:2101.11735](#)] [INSPIRE].
- [21] D.J.E. Marsh, *Axion Cosmology*, *Phys. Rept.* **643** (2016) 1 [[arXiv:1510.07633](#)] [INSPIRE].

- [22] W. Hu, R. Barkana and A. Gruzinov, *Cold and fuzzy dark matter*, *Phys. Rev. Lett.* **85** (2000) 1158 [[astro-ph/0003365](#)] [[INSPIRE](#)].
- [23] S.-J. Sin, *Late time cosmological phase transition and galactic halo as Bose liquid*, *Phys. Rev. D* **50** (1994) 3650 [[hep-ph/9205208](#)] [[INSPIRE](#)].
- [24] P.J.E. Peebles, *Fluid dark matter*, *Astrophys. J. Lett.* **534** (2000) L127 [[astro-ph/0002495](#)] [[INSPIRE](#)].
- [25] W.H. Press, B.S. Ryden and D.N. Spergel, *Single Mechanism for Generating Large Scale Structure and Providing Dark Missing Matter*, *Phys. Rev. Lett.* **64** (1990) 1084 [[INSPIRE](#)].
- [26] M.R. Baldeschi, R. Ruffini and G.B. Gelmini, *On massive fermions and bosons in galactic halos*, *Phys. Lett. B* **122** (1983) 221 [[INSPIRE](#)].
- [27] J. Goodman, *Repulsive dark matter*, *New Astron.* **5** (2000) 103 [[astro-ph/0003018](#)] [[INSPIRE](#)].
- [28] A. Arbey, J. Lesgourgues and P. Salati, *Galactic halos of fluid dark matter*, *Phys. Rev. D* **68** (2003) 023511 [[astro-ph/0301533](#)] [[INSPIRE](#)].
- [29] L. Amendola and R. Barbieri, *Dark matter from an ultra-light pseudo-Goldstone-boson*, *Phys. Lett. B* **642** (2006) 192 [[hep-ph/0509257](#)] [[INSPIRE](#)].
- [30] P.-H. Chavanis, *Mass-radius relation of Newtonian self-gravitating Bose-Einstein condensates with short-range interactions. I. Analytical results*, *Phys. Rev. D* **84** (2011) 043531 [[arXiv:1103.2050](#)] [[INSPIRE](#)].
- [31] A. Suarez and T. Matos, *Structure Formation with Scalar Field Dark Matter: The Fluid Approach*, *Mon. Not. Roy. Astron. Soc.* **416** (2011) 87 [[arXiv:1101.4039](#)] [[INSPIRE](#)].
- [32] L. Berezhiani and J. Khoury, *Theory of dark matter superfluidity*, *Phys. Rev. D* **92** (2015) 103510 [[arXiv:1507.01019](#)] [[INSPIRE](#)].
- [33] J.J. Fan, *Ultralight Repulsive Dark Matter and BEC*, *Phys. Dark Univ.* **14** (2016) 84 [[arXiv:1603.06580](#)] [[INSPIRE](#)].
- [34] M. Blennow et al., *Neutrino Portals to Dark Matter*, *Eur. Phys. J. C* **79** (2019) 555 [[arXiv:1903.00006](#)] [[INSPIRE](#)].
- [35] A. Berlin, *Neutrino Oscillations as a Probe of Light Scalar Dark Matter*, *Phys. Rev. Lett.* **117** (2016) 231801 [[arXiv:1608.01307](#)] [[INSPIRE](#)].
- [36] A. Dev, P.A.N. Machado and P. Martínez-Miravé, *Signatures of ultralight dark matter in neutrino oscillation experiments*, *JHEP* **01** (2021) 094 [[arXiv:2007.03590](#)] [[INSPIRE](#)].
- [37] G. Krnjaic, P.A.N. Machado and L. Necib, *Distorted neutrino oscillations from time varying cosmic fields*, *Phys. Rev. D* **97** (2018) 075017 [[arXiv:1705.06740](#)] [[INSPIRE](#)].
- [38] V. Barger, P. Huber and D. Marfatia, *Solar mass-varying neutrino oscillations*, *Phys. Rev. Lett.* **95** (2005) 211802 [[hep-ph/0502196](#)] [[INSPIRE](#)].
- [39] V. Brdar et al., *Fuzzy dark matter and nonstandard neutrino interactions*, *Phys. Rev. D* **97** (2018) 043001 [[arXiv:1705.09455](#)] [[INSPIRE](#)].
- [40] M. Losada, Y. Nir, G. Perez and Y. Shpilman, *Probing scalar dark matter oscillations with neutrino oscillations*, *JHEP* **04** (2022) 030 [[arXiv:2107.10865](#)] [[INSPIRE](#)].
- [41] F. Capozzi, I.M. Shoemaker and L. Vecchi, *Neutrino Oscillations in Dark Backgrounds*, *JCAP* **07** (2018) 004 [[arXiv:1804.05117](#)] [[INSPIRE](#)].
- [42] A. Cheek, L. Visinelli and H.-Y. Zhang, *Testing the Dark Origin of Neutrino Masses with Oscillation Experiments*, *Phys. Rev. Lett.* **135** (2025) 031801 [[arXiv:2503.08439](#)] [[INSPIRE](#)].

- [43] Y.L. ChoeJo, Y. Kim and H.-S. Lee, *Dirac-Majorana neutrino type oscillation induced by a wave dark matter*, *Phys. Rev. D* **108** (2023) 095028 [[arXiv:2305.16900](#)] [[INSPIRE](#)].
- [44] E.J. Chun, *Neutrino Transition in Dark Matter*, [arXiv:2112.05057](#) [[INSPIRE](#)].
- [45] K.-Y. Choi, E.J. Chun and J. Kim, *Neutrino Oscillations in Dark Matter*, *Phys. Dark Univ.* **30** (2020) 100606 [[arXiv:1909.10478](#)] [[INSPIRE](#)].
- [46] J. Liao, D. Marfatia and K. Whisnant, *Light scalar dark matter at neutrino oscillation experiments*, *JHEP* **04** (2018) 136 [[arXiv:1803.01773](#)] [[INSPIRE](#)].
- [47] S.-F. Ge and H. Murayama, *Apparent CPT Violation in Neutrino Oscillation from Dark Non-Standard Interactions*, [arXiv:1904.02518](#) [[INSPIRE](#)].
- [48] C. Murgui and R. Plestid, *Coleman-Weinberg dynamics of ultralight scalar dark matter and GeV-scale right-handed neutrinos*, *JHEP* **08** (2024) 168 [[arXiv:2306.13799](#)] [[INSPIRE](#)].
- [49] S.-F. Ge, C.-F. Kong and A.Y. Smirnov, *Testing the Origins of Neutrino Mass with Supernova-Neutrino Time Delay*, *Phys. Rev. Lett.* **133** (2024) 121802 [[arXiv:2404.17352](#)] [[INSPIRE](#)].
- [50] M.M. Reynoso and O.A. Sampayo, *Propagation of high-energy neutrinos in a background of ultralight scalar dark matter*, *Astropart. Phys.* **82** (2016) 10 [[arXiv:1605.09671](#)] [[INSPIRE](#)].
- [51] M.M. Reynoso, O.A. Sampayo and A.M. Carulli, *Neutrino interactions with ultralight axion-like dark matter*, *Eur. Phys. J. C* **82** (2022) 274 [[arXiv:2203.11642](#)] [[INSPIRE](#)].
- [52] G. Lambiase and T.K. Poddar, *Pulsar kicks in ultralight dark matter background induced by neutrino oscillation*, *JCAP* **01** (2024) 069 [[arXiv:2307.05229](#)] [[INSPIRE](#)].
- [53] S. Pandey, S. Karmakar and S. Rakshit, *Interactions of astrophysical neutrinos with dark matter: a model building perspective*, *JHEP* **11** (2019) 215 [Erratum *ibid.* **11** (2021) 215] [[arXiv:1810.04203](#)] [[INSPIRE](#)].
- [54] Y. Farzan and S. Palomares-Ruiz, *Flavor of cosmic neutrinos preserved by ultralight dark matter*, *Phys. Rev. D* **99** (2019) 051702 [[arXiv:1810.00892](#)] [[INSPIRE](#)].
- [55] G.-Y. Huang and N. Nath, *Neutrinophilic Axion-Like Dark Matter*, *Eur. Phys. J. C* **78** (2018) 922 [[arXiv:1809.01111](#)] [[INSPIRE](#)].
- [56] G.-Y. Huang and N. Nath, *Neutrino meets ultralight dark matter: $0\nu\beta\beta$ decay and cosmology*, *JCAP* **05** (2022) 034 [[arXiv:2111.08732](#)] [[INSPIRE](#)].
- [57] G.-Y. Huang, M. Lindner, P. Martínez-Miravé and M. Sen, *Cosmology-friendly time-varying neutrino masses via the sterile neutrino portal*, *Phys. Rev. D* **106** (2022) 033004 [[arXiv:2205.08431](#)] [[INSPIRE](#)].
- [58] A. Dev, G. Krnjaic, P. Machado and H. Ramani, *Constraining feeble neutrino interactions with ultralight dark matter*, *Phys. Rev. D* **107** (2023) 035006 [[arXiv:2205.06821](#)] [[INSPIRE](#)].
- [59] R. Plestid and S. Tevosyan, *The cosmology of ultralight scalar dark matter coupled to right-handed neutrinos*, *JHEP* **07** (2025) 012 [[arXiv:2409.17396](#)] [[INSPIRE](#)].
- [60] J. Venzor, A. Pérez-Lorenzana and J. De-Santiago, *Bounds on neutrino-scalar nonstandard interactions from big bang nucleosynthesis*, *Phys. Rev. D* **103** (2021) 043534 [[arXiv:2009.08104](#)] [[INSPIRE](#)].
- [61] H. Davoudiasl, G. Mohlabeng and M. Sullivan, *Galactic Dark Matter Population as the Source of Neutrino Masses*, *Phys. Rev. D* **98** (2018) 021301 [[arXiv:1803.00012](#)] [[INSPIRE](#)].

- [62] A.Y. Smirnov and V.B. Valera, *Resonance refraction and neutrino oscillations*, *JHEP* **09** (2021) 177 [[arXiv:2106.13829](#)] [[INSPIRE](#)].
- [63] P. Martínez-Miravé, Y.F. Perez-Gonzalez and M. Sen, *Effects of neutrino-ultralight dark matter interaction on the cosmic neutrino background*, *Phys. Rev. D* **110** (2024) 055005 [[arXiv:2406.01682](#)] [[INSPIRE](#)].
- [64] Y. Kim and H.-S. Lee, *Oscillating scalar potential and its implications for cosmic neutrino background searches*, *JHEP* **07** (2025) 269 [[arXiv:2503.04949](#)] [[INSPIRE](#)].
- [65] K.S. Babu, G. Chauhan and P.S. Bhupal Dev, *Neutrino nonstandard interactions via light scalars in the Earth, Sun, supernovae, and the early Universe*, *Phys. Rev. D* **101** (2020) 095029 [[arXiv:1912.13488](#)] [[INSPIRE](#)].
- [66] M. Sen and A.Y. Smirnov, *Refractive neutrino masses, ultralight dark matter and cosmology*, *JCAP* **01** (2024) 040 [[arXiv:2306.15718](#)] [[INSPIRE](#)].
- [67] M. Sen and A.Y. Smirnov, *Neutrinos with refractive masses and the DESI baryon acoustic oscillation results*, *Phys. Rev. D* **111** (2025) 103048 [[arXiv:2407.02462](#)] [[INSPIRE](#)].
- [68] J.-W. Lee, *Neutrino mass and ultralight dark matter mass from the Higgs mechanism*, [arXiv:2410.02842](#) [[INSPIRE](#)].
- [69] E. Ma, *Common origin of neutrino mass, dark matter, and baryogenesis*, *Mod. Phys. Lett. A* **21** (2006) 1777 [[hep-ph/0605180](#)] [[INSPIRE](#)].
- [70] A. Berlin and D. Hooper, *Axion-Assisted Production of Sterile Neutrino Dark Matter*, *Phys. Rev. D* **95** (2017) 075017 [[arXiv:1610.03849](#)] [[INSPIRE](#)].
- [71] G. Lambiase, T.K. Poddar and L. Visinelli, *Impact of the cosmic neutrino background on black hole superradiance*, *Phys. Rev. D* **112** (2025) 016010 [[arXiv:2503.02940](#)] [[INSPIRE](#)].
- [72] R.F. Sawyer, *Do neutrinos have mass only within matter?*, *Phys. Lett. B* **448** (1999) 174 [[hep-ph/9809348](#)] [[INSPIRE](#)].
- [73] K.-Y. Choi, E.J. Chun and J. Kim, *Dispersion of neutrinos in a medium*, [arXiv:2012.09474](#) [[INSPIRE](#)].
- [74] T. Bertólez-Martínez et al., *Origin of cosmological neutrino mass bounds: background versus perturbations*, *JCAP* **06** (2025) 058 [[arXiv:2411.14524](#)] [[INSPIRE](#)].
- [75] J.E. Moody and F. Wilczek, *New Macroscopic Forces?*, *Phys. Rev. D* **30** (1984) 130 [[INSPIRE](#)].
- [76] J.E. Kim, *Light Pseudoscalars, Particle Physics and Cosmology*, *Phys. Rept.* **150** (1987) 1 [[INSPIRE](#)].
- [77] L. Parker and D. Toms, *Quantum Field Theory in Curved Spacetime: Quantized Fields and Gravity*, Cambridge Monographs on Mathematical Physics, Cambridge University Press (2009) [[DOI:10.1017/cbo9780511813924](#)].
- [78] I. Esteban and J. Salvado, *Long Range Interactions in Cosmology: Implications for Neutrinos*, *JCAP* **05** (2021) 036 [[arXiv:2101.05804](#)] [[INSPIRE](#)].
- [79] A.Y. Smirnov and X.-J. Xu, *Neutrino bound states and bound systems*, *JHEP* **08** (2022) 170 [[arXiv:2201.00939](#)] [[INSPIRE](#)].
- [80] C. Gao and A. Stebbins, *Structure of stellar remnants with coupling to a light scalar*, *JCAP* **07** (2022) 025 [[arXiv:2110.07012](#)] [[INSPIRE](#)].
- [81] C.-P. Ma and E. Bertschinger, *Cosmological perturbation theory in the synchronous and conformal Newtonian gauges*, *Astrophys. J.* **455** (1995) 7 [[astro-ph/9506072](#)] [[INSPIRE](#)].

- [82] L.D. Landau and E.M. Lifshitz, *Mechanics, Third Edition: Volume 1 (Course of Theoretical Physics)*, Butterworth-Heinemann (1976).
- [83] J. Lesgourgues, *The Cosmic Linear Anisotropy Solving System (CLASS) I: Overview*, [arXiv:1104.2932](#) [INSPIRE].
- [84] D. Blas, J. Lesgourgues and T. Tram, *The Cosmic Linear Anisotropy Solving System (CLASS) II: Approximation schemes*, *JCAP* **07** (2011) 034 [[arXiv:1104.2933](#)] [INSPIRE].
- [85] J. Lesgourgues, *The Cosmic Linear Anisotropy Solving System (CLASS) III: Comparison with CAMB for LambdaCDM*, [arXiv:1104.2934](#) [INSPIRE].
- [86] J. Lesgourgues and T. Tram, *The Cosmic Linear Anisotropy Solving System (CLASS) IV: efficient implementation of non-cold relics*, *JCAP* **09** (2011) 032 [[arXiv:1104.2935](#)] [INSPIRE].
- [87] PLANCK collaboration, *Planck 2018 results. VI. Cosmological parameters*, *Astron. Astrophys.* **641** (2020) A6 [*Erratum ibid.* **652** (2021) C4] [[arXiv:1807.06209](#)] [INSPIRE].
- [88] C. Pitrou, A. Coc, J.-P. Uzan and E. Vangioni, *Precision big bang nucleosynthesis with improved Helium-4 predictions*, *Phys. Rept.* **754** (2018) 1 [[arXiv:1801.08023](#)] [INSPIRE].
- [89] PARTICLE DATA GROUP collaboration, *Review of particle physics*, *Phys. Rev. D* **110** (2024) 030001 [INSPIRE].
- [90] A.-K. Burns, T.M.P. Tait and M. Valli, *PRyMordial: the first three minutes, within and beyond the standard model*, *Eur. Phys. J. C* **84** (2024) 86 [[arXiv:2307.07061](#)] [INSPIRE].
- [91] E.C.G. Sudarshan, *Equivalence of semiclassical and quantum mechanical descriptions of statistical light beams*, *Phys. Rev. Lett.* **10** (1963) 277 [INSPIRE].
- [92] R.J. Glauber, *Coherent and incoherent states of the radiation field*, *Phys. Rev.* **131** (1963) 2766 [INSPIRE].
- [93] R.J. Glauber, *The quantum theory of optical coherence*, *Phys. Rev.* **130** (1963) 2529 [INSPIRE].
- [94] M.E. Peskin and D.V. Schroeder, *An introduction to quantum field theory*, Addison-Wesley, Reading, U.S.A. (1995) [DOI:10.1201/9780429503559] [INSPIRE].
- [95] F. Halzen and A.D. Martin, *Quarks and leptons: an introductory course in modern particle physics*, Wiley (1984) [INSPIRE].
- [96] A.W. Brookfield, C. van de Bruck, D.F. Mota and D. Tocchini-Valentini, *Cosmology of mass-varying neutrinos driven by quintessence: theory and observations*, *Phys. Rev. D* **73** (2006) 083515 [*Erratum ibid.* **76** (2007) 049901] [[astro-ph/0512367](#)] [INSPIRE].